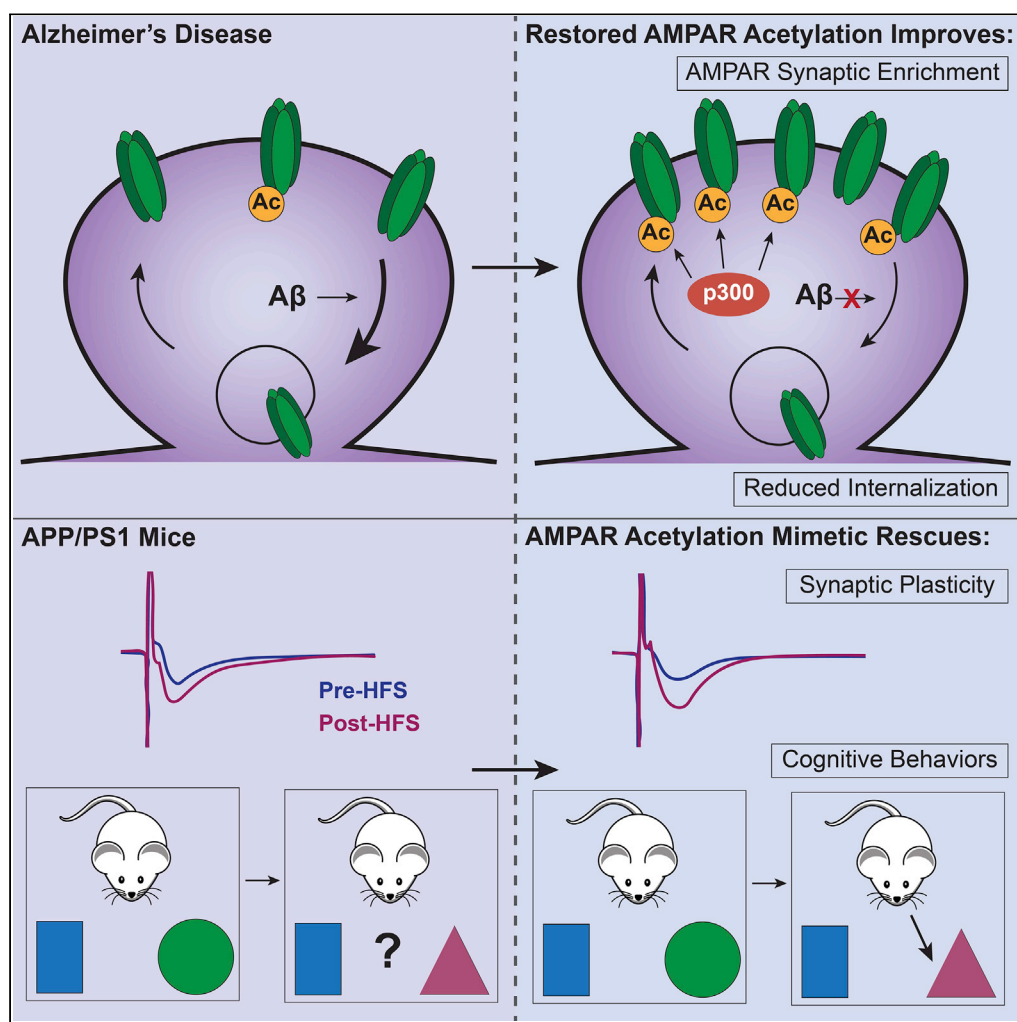**Article**

Acetylation of AMPA Receptors Regulates Receptor Trafficking and Rescues Memory Deficits in Alzheimer's Disease

Margaret O'Connor, Yang-Ping Shentu, Guan Wang, ..., Xiao-Chuan Wang, Rong Liu, Heng-Ye Man

rong.liu@hust.edu.cn (R.L.)
hman@bu.edu (H.-Y.M.)

HIGHLIGHTS

AMPAR acetylation is reduced in AD brain and neurons with Aβ incubation

p300 is the acetyltransferase for AMPAR acetylation

Up-regulation of AMPAR acetylation in neurons blocks Aβ-induced receptor internalization

Expression of GluA1 acetylation mimetic rescues cognitive deficits in APP/PS1 mice

iScience

Article

Acetylation of AMPA Receptors Regulates Receptor Trafficking and Rescues Memory Deficits in Alzheimer's Disease

Margaret O'Connor,[1,6] Yang-Ping Shentu,[2,3,6] Guan Wang,[1] Wen-Ting Hu,[2] Zhen-Dong Xu,[2] Xiao-Chuan Wang,[2] Rong Liu,[2,*] and Heng-Ye Man[1,4,5,7,*]

SUMMARY

In Alzheimer's disease (AD), decreases in the amount and synaptic localization of AMPA receptors (AMPARs) result in weakened synaptic activity and dysfunction in synaptic plasticity, leading to impairments in cognitive functions. We have previously found that AMPARs are subject to lysine acetylation, resulting in higher AMPAR stability and protein accumulation. Here we report that AMPAR acetylation was significantly reduced in AD and neurons with Aβ incubation. We identified p300 as the acetyltransferase responsible for AMPAR acetylation and found that enhancing GluA1 acetylation ameliorated Aβ-induced reductions in total and cell-surface AMPARs. Importantly, expression of acetylation mimetic GluA1 (GluA1-4KQ) in APP/PS1 mice rescued impairments in synaptic plasticity and memory. These findings indicate that Aβ-induced reduction in AMPAR acetylation and stability contributes to synaptopathy and memory deficiency in AD, suggesting that AMPAR acetylation may be an effective molecular target for AD therapeutics.

INTRODUCTION

Alzheimer's disease (AD) is the most common form of dementia characterized by impairments in learning and memory. A key hallmark of AD is the accumulation of amyloid-β (Aβ), which has been shown to cause loss of dendritic spines and dysregulation in synaptic functions, such as basal transmission and synaptic plasticity (Forner et al., 2019; Palop and Mucke, 2010; Rajmohan and Reddy, 2017; Selkoe, 2002; Sheng et al., 2012; Yu and Lu, 2012). Evidence suggests these impairments in synaptic function are an early pathology, which ultimately lead to the cognitive failures observed in AD (Baglietto-Vargas et al., 2018; Chen et al., 2000; Li et al., 2011; Ma and Klann, 2012; Oddo et al., 2003; Selkoe and Hardy, 2016).

AMPA receptors (AMPARs) mediate most of the excitatory synaptic transmission that underlies higher brain functions, including learning and memory. A change in the synaptic expression of AMPARs is the key mechanism underlying synaptic plasticity, the molecular basis for learning and memory. An increase in surface AMPARs through exocytosis leads to the expression of long-term potentiation (LTP), whereas internalization of AMPARs causes long-term depression (LTD) (Chidambaram et al., 2019; Collingridge et al., 2004; Derkach et al., 2007; Ju and Zhou, 2018; Kopec et al., 2006; Lledo et al., 1998; Lüscher et al., 1999; Makino and Malinow, 2009; Malinow and Malenka, 2002; Shepherd and Huganir, 2007; Song and Huganir, 2002). Consistent with impairments in synaptic function, a reduction in AMPARs has been observed in the brains of both human patients with AD and mouse models of AD (Armstrong et al., 1994; Cantanelli et al., 2014; Carter et al., 2004; Chang et al., 2006; D'Amelio et al., 2011; Dewar et al., 1991; Du et al., 2020; Gao et al., 2016; Gong et al., 2009; Jacob et al., 2007; Monteiro-Fernandes et al., 2020; Samra and Ramtahal, 2012; Thorns et al., 1997; Wakabayashi et al., 1999; Yasuda et al., 1995). In line with this, incubation of neurons with Aβ results in down-regulation in AMPAR amounts (Guntupalli et al., 2016; Miyamoto et al., 2016; Parameshwaran et al., 2008; Thomas et al., 2017; Wisniewski et al., 2011; Yu and Lu, 2012; Zhang et al., 2018).

The abundance of AMPARs in the post-synaptic domain is regulated by dynamic receptor trafficking. Enhanced receptor internalization and an ultimate reduction in AMPAR synaptic accumulation has been shown to be an early pathological feature of AD (Almeida et al., 2005; Baglietto-Vargas et al., 2018; Hsieh

[1]Department of Biology, Boston University, 5 Cummington Mall, Boston, MA 02215, USA

[2]Department of Pathophysiology, School of Basic Medicine, Tongji Medical College, Huazhong University of Science and Technology, Wuhan 430030, China

[3]Department of Pathology, the First Affiliated Hospital of Wenzhou Medical University, Wenzhou, China

[4]Department of Pharmacology & Experimental Therapeutics, Boston University School of Medicine, 72 East Concord St., L-603, Boston, MA 02118, USA

[5]Center for Systems Neuroscience, Boston University, 610 Commonwealth Avenue, Boston, MA, USA

[6]These authors contributed equally

[7]Lead Contact

*Correspondence: rong.liu@hust.edu.cn (R.L.), hman@bu.edu (H.-Y.M.)

https://doi.org/10.1016/j.isci. 2020.101465

et al., 2006; Li et al., 2019; Zhao et al., 2010). Overexpression of amyloid precursor protein (APP) or application of soluble oligomeric Aβ results in a reduction in surface expression of AMPARs (Alfonso et al., 2014; Gu et al., 2009; Miller et al., 2014; Roselli et al., 2005; Tanaka et al., 2019; Zhang et al., 2011) likely due to endocytosis of AMPARs from the synaptic surface (Hsieh et al., 2006; Miñano-Molina et al., 2011; Wang et al., 2011; Zhang et al., 2017). The reduced stability of AMPARs may be a major contributing factor to the pathology of AD.

In AD, the reduction in AMPAR seems to result from reduced receptor stability. Indeed, treatment with Aβ increased AMPAR mobility (Opazo et al., 2018) and, in the presence of cycloheximide, shortened AMPAR half-life (Zhang et al., 2018). Studies have demonstrated that ubiquitination is a primary regulatory mechanism contributing to AMPAR stability (Guntupalli et al., 2017; Rodrigues et al., 2016; Zhang et al., 2018). AMPARs are subject to ubiquitination via the E3 ligase Nedd4 (Hou et al., 2011; Lin et al., 2011; Rodrigues et al., 2016; Schwarz et al., 2010) and deubiquitination by the deubiquitinase USP46 (Huo et al., 2015). Plasma membrane-inserted AMPARs are preferentially targeted for ubiquitination (Lin et al., 2011), leading to receptor internalization and subsequent proteasomal degradation (Goo et al., 2015; Hou et al., 2011; Jarzylo and Man, 2012; Zhang et al., 2009).

We have recently demonstrated that AMPARs are also subject to lysine acetylation, a regulation that competes with ubiquitination because both processes target lysine residues. Acetylation confers AMPARs with higher levels of stability due to a suppression in AMPAR internalization and degradation (Wang et al., 2017). We have shown that inhibition of the AMPAR deacetylase, SIRT2, causes enhanced AMPAR acetylation and increased AMPAR accumulation at synapses (Wang et al., 2017). Because AMPAR reduction is a crucial first step leading to the cognitive deficits in AD, restoration of AMPARs at the synapse is predicted to improve synaptic strength and cognitive function in AD.

In this study, we find that AMPAR acetylation is altered under AD conditions. In Aβ-incubated neurons, and in brains of transgenic AD mice and patients with AD, AMPARs show marked reduction in acetylation. We show that up-regulation of AMPAR acetylation leads to a suppression in AMPAR internalization and an increase in total AMPAR amount. We identify p300 as the acetyltransferase responsible for AMPAR acetylation and find that activation of p300, or inhibition of AMPAR deacetylase SIRT2, results in an increase in AMPAR acetylation and blocks the Aβ-induced reduction in surface AMPAR expression. Importantly, we found that hippocampal expression of an acetylation mimetic GluA1 was able to restore synaptic plasticity and rescue cognitive deficits in the Tg (APPswe, PSEN1dE9)85Dbo (APP/PS1) mouse model. Together, these findings provide insights into the importance of AMPAR acetylation in the pathogenesis of cognitive dysfunction in AD.

RESULTS

Aβ Induces a Reduction in AMPAR Acetylation

Our studies and the work of others have shown that AMPAR levels are reduced in AD (Armstrong et al., 1994; Carter et al., 2004; Dewar et al., 1991; Gong et al., 2009; Thorns et al., 1997; Yasuda et al., 1995; Zhang et al., 2018). In AD brains and Aβ-treated neurons, ubiquitination of AMPARs is up-regulated (Guntupalli et al., 2017; Rodrigues et al., 2016; Zhang et al., 2018), and studies have demonstrated proteasomal degradation of ubiquitinated AMPARs (Huo et al., 2015; Jarzylo and Man, 2012; Lin et al., 2011). Recently, we found that AMPARs are subject to another form of protein modification, i.e., acetylation, a modification that opposes receptor ubiquitination and functions to stabilize AMPARs (Wang et al., 2017). We therefore wondered whether this modification of AMPARs is altered in AD conditions, contributing to the aberrance in receptor expression. To this end, we first used immunostaining to confirm the effect of Aβ oligomers on the abundance of AMPAR expression. DIV 15 cultured rat hippocampal neurons were treated with Aβ (1 μM) for 24 h and labeled with specific antibodies against AMPAR subunit GluA1. Immunostaining against the GluA1 N terminus under non-permeant conditions showed a reduction in the intensity of surface GluA1 puncta, and antibodies against the GluA1 C terminus under permeant conditions showed a similar reduction in total levels of GluA1 (Figures 1A and 1B). To examine specifically the expression level of AMPARs at the synaptic sites, we purified synaptosomes from cultured cortical neurons. We found that the Aβ treatment resulted in a 62% reduction in the amount of GluA1 in the synaptosome, comparable with an overall 65% reduction from total cell lysate (Figures 1C and 1D). In addition, we found that Aβ treatment did not affect the levels of PSD95 (Figure 1E). These findings indicate that Aβ incubation leads to a down-regulation of synaptic AMPARs in neurons.
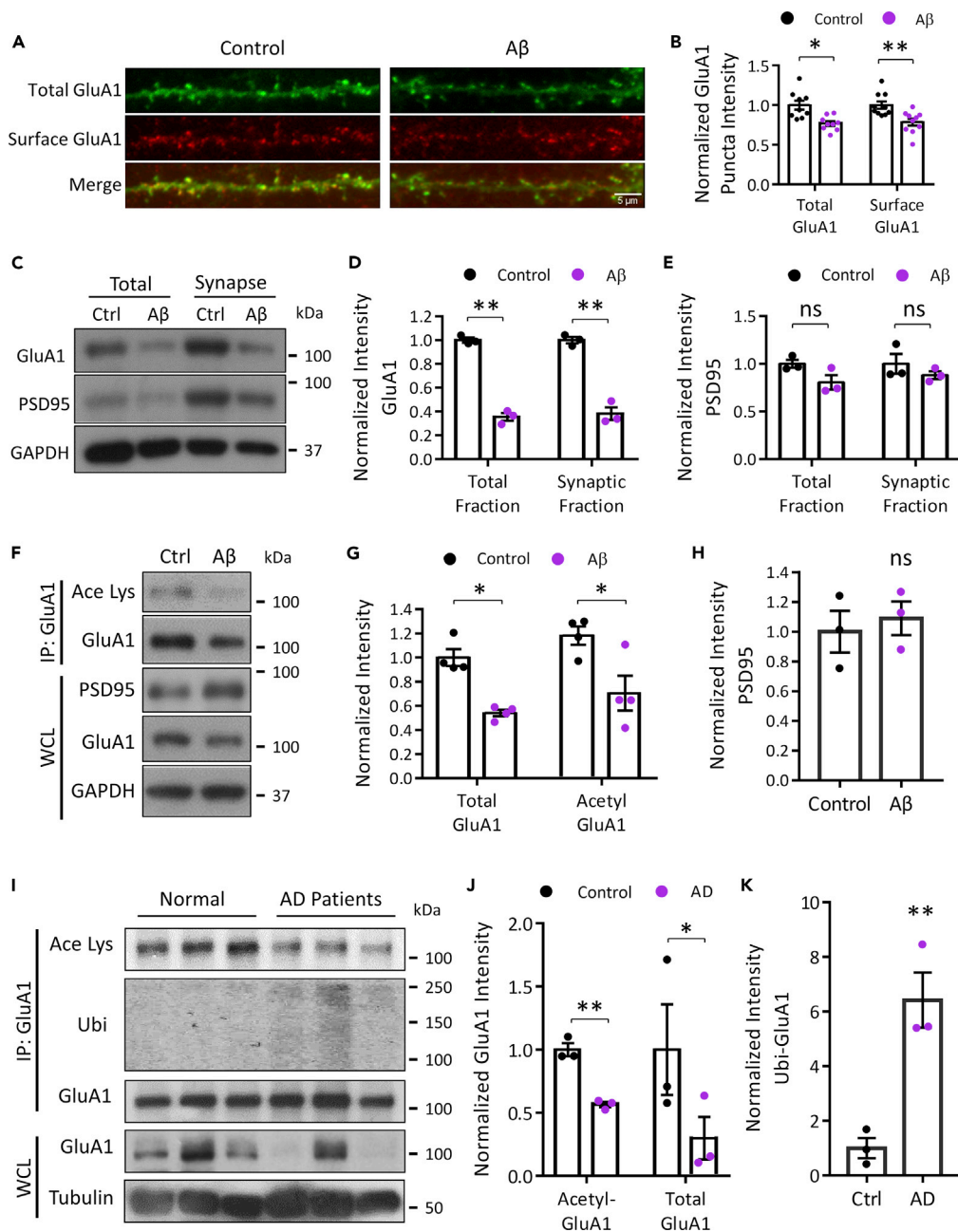
Figure 1. Aβ Treatment Induces a Reduction in AMPAR Acetylation

(A) Hippocampal neurons were treated with Aβ (1 μM) for 24 h and probed for synaptic GluA1 using immunocytochemistry (Total GluA1, green; Surface GluA1, red) (scale bar, 5 μm).

(B) Quantitative analysis of the GluA1 puncta intensity showed a decrease in both surface and total intensities (Ctrl, $n = 10$ cells, 548 puncta; Aβ, $n = 11$ cells, 511 puncta).

(C) Synaptosome purification of cultured cortical neurons incubated with Aβ ($n = 3$ experiments).

(D) Quantification showed a decrease in synaptically localized, as well as total, GluA1 levels.

(E) Quantification shows no change in PSD95 levels.

(F) GluA1 acetylation levels were assessed via acetylation assays using cultured cortical neurons incubated with Aβ ($n = 4$ experiments).

(G) Quantitative analysis showed that application of Aβ reduced acetylated and total GluA1 levels. GluA1 acetylation was measured by normalizing the acetyl-lysine signal to the amount of GluA1 in IP.

(H) Quantification shows no change in PSD95 levels.

(I) Acetylation assays from prefrontal cortical brain homogenates from AD patient and healthy control brains ($n = 3$ brains).

Figure 1. *Continued*
(J) Quantification showed reduced acetylation of GluA1 in AD patients' brains compared with those of controls.
(K) Quantification showed a significant increase in GluA1 ubiquitination in AD brains compared with those of controls.
*p<0.05, **p<0.01. Data are mean ± SEM.

We wondered whether AMPAR acetylation plays a role in Aβ-induced AMPAR down-regulation. Using DIV 15 primary cortical neurons treated with Aβ (1 μM) for 24 h, we isolated AMPAR GluA1 subunits via immunoprecipitation and probed western blots with antibodies specific for lysine acetylation (Inuzuka et al., 2012; Wang et al., 2017). We found that, compared with the control, incubation with Aβ resulted in a significant reduction in acetylation signal in precipitated GluA1 (Figures 1F and 1G). There was no significant difference in PSD95 levels (Figure 1H). To further determine the state of AMPAR acetylation in AD, we examined lysates from postmortem AD patient brains. GluA1 was precipitated from the prefrontal cortex lysates from patients and healthy controls. In line with our findings from Aβ-treated neurons, the AD patient brain homogenates showed a consistent decrease in the extent of GluA1 acetylation compared with the non-AD controls (Figures 1I and 1J). We also observed a dramatic increase in GluA1 ubiquitination (Figure 1K). Together these results demonstrate that AMPAR acetylation is decreased *in vitro* in Aβ-treated neurons and *ex vivo* in human AD brains.

The Acetyltransferase p300 Causes GluA1 Acetylation

Our previous work has identified SIRT2 as the deacetylase responsible for the deacetylation of GluA1 (Wang et al., 2017); however, the enzyme(s) responsible for AMPAR acetylation remains unknown. We therefore sought to identify the acetyltransferase that catalyzes the conjugation of the acetyl group to the lysine residues at GluA1 C terminus (GluA1ct). To this end, we purified GST-tagged GluA1ct and incubated it with several acetyltransferases, including PCAF, p300, CBP, and GCN5, individually (Figure 2A). Interestingly, when the GluA1ct was probed for lysine acetylation, we observed a marked increase in GluA1 acetylation in assays that contained p300 and a trend of increase with the p300 homolog CBP (Figure 2B). However, this was not observed in assays containing PCAF or GCN5. This result indicates a specific role for the p300 family of acetyltransferases on AMPAR acetylation. p300 is well known for its role in histone acetylation for the regulation of gene expression, but it is also localized in the cytoplasm (Dancy and Cole, 2015; Kwok et al., 2006; Rotte et al., 2013; Shi et al., 2009). It is therefore possible for the endogenous p300 to acetylate AMPARs in neurons. To confirm the effect of p300 on AMPAR acetylation *in vivo*, we incubated primary cortical neurons with either the p300 inhibitor C646 (20 μM) (Bowers et al., 2010) or the p300 acetyltransferase activator CTPB (20 μM) (Balasubramanyam et al., 2003), for 24 h, and immunoprecipitated GluA1 for acetylation assays. Indeed, inhibition of p300 by C646 caused a decrease in GluA1 acetylation, whereas activation of p300 by CTPB increased acetylation of GluA1 (Figure 2C). Because an acetylation event often antagonizes protein ubiquitination owing to competition for the same lysine residues, we examined changes in GluA1 ubiquitination. As expected, inhibition of p300 led to an increase, whereas activation of p300 by CTPB caused a decrease in the level of GluA1 ubiquitination (Figure 2C).

p300-Mediated Acetylation Leads to AMPAR Stabilization

Acetylation has been shown to cause stabilization of membrane proteins and expansion of protein's half-life (Alaei et al., 2018; Caron et al., 2005; Drazic et al., 2016; Mak et al., 2014). To determine whether acetylation by p300 confers AMPAR with enhanced stability, we transfected p300, together with GFP, in primary hippocampal neurons. Immunostainings showed an overexpression of p300 led to an increase in the total GluA1 puncta intensity (Figures 2D and 2E). In addition, we transfected p300 with GFP-GluA1 into HEK293T cells and measured the total GluA1 levels by western blotting analysis. In line with our findings in neurons, expression of p300 led to an increase in total GluA1 levels compared with the pcDNA control, whereas expression of PCAF did not affect the amount of GluA1 (Figures 2F and 2G). These results showed that p300 acetyltransferase activity facilitates AMPAR acetylation and stabilization, supporting that p300 functions as the acetyltransferase for AMPAR acetylation.

The Lysine Residues in the GluA1 C-Terminal Tail Are the Targets for p300-Mediated AMPAR Acetylation

Because the acetyl group is conjugated to lysine residues of the substrate during acetylation, the four lysine residues located in the GluA1 C terminus are potential candidate sites for p300-mediated acetylation. To confirm the acetylation sites, we mutated all four of the lysine residues in GluA1ct to arginine (GluA1-4KR). Arginine's side group mimics the charge of lysine's side group thus preserving structural integrity but is
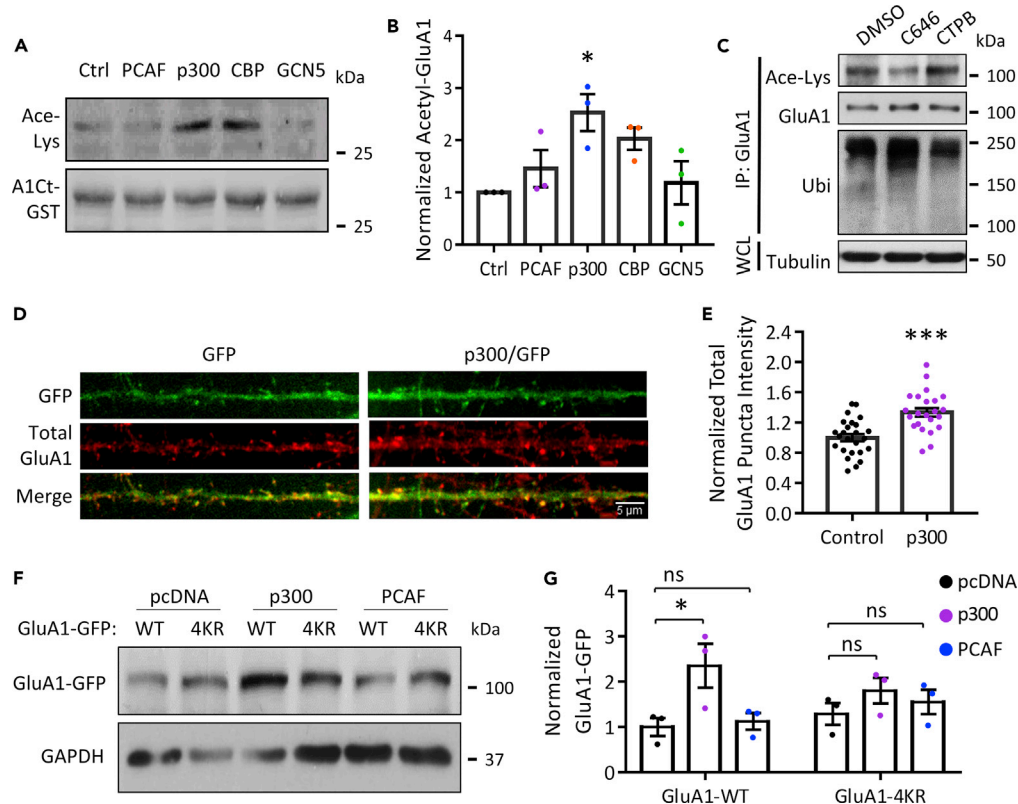
Figure 2. Acetyltransferase p300 Acetylates and Stabilizes AMPARs

(A) Acetylation assays from *in vitro* reactions with purified acetyltransferases.

(B) Quantification shows that incubation with p300, but not CBP, PCAF, or GCN5, increased GluA1 acetylation. (*n* = 3 experiments).

(C) Inhibition of p300 acetyltransferase activity by C646 (40 μM, 4 h) led to reduced acetylation, whereas activation by CTPB (20 μM, 4 h) led to increased acetylation.

(D) GluA1 puncta levels were assessed by immunocytochemistry following overexpression of p300 (Total GluA1, red) (scale bar, 5 μm).

(E) Quantitative analysis showed overexpression of p300 increased total GluA1 puncta intensity. (Ctrl, *n* = 25 cells, 2,407 puncta; p300, *n* = 23 cells, 2,164 puncta).

(F and G) In HEK293T cells, overexpression of p300 increases GluA1 intensity. Additionally, expression of GluA1-4KR mutant abolishes p300-induced GluA1-WT up-regulation, indicating the lysine-dependence of p300 effect (*n* = 3 experiments).

*p<0.05, ***p<0.001. Data are mean ± SEM.

incapable of being acetylated (Inuzuka et al., 2012). We transfected HEK293 cells with GFP-GluA1-4KR, together with p300, PCAF, or control vector pcDNA, respectively, and used the cell lysates to assess GluA1 protein levels to evaluate p300 effects on GluA1-4KR accumulation. Indeed, the previously observed increase in GluA1-WT levels from p300 overexpression was abolished in cells expressing GFP-GluA1-4KR (Figures 2F and 2G), indicating that the C-terminal lysine residues are required for p300-mediated GluA1 acetylation and stabilization.

Acetylation of GluA1 Suppresses the Aβ-Induced Reduction of AMPAR Amount and Synaptic Accumulation

Because acetylation reduces the rate of AMPAR turnover and increases AMPAR accumulation in neurons (Wang et al., 2017), we hypothesize that acetylation should lead to suppression of Aβ-induced AMPAR degradation. To test this idea, we incubated DIV 15 hippocampal neurons with Aβ alone, or with the SIRT2 inhibitor B2, for 24 h. We found that treatment with B2 (2 μM) alone resulted in an increase in both total and surface GluA1 (Figures 3A–3C). Importantly, Aβ-induced reduction in AMPARs was blocked by co-incubation with B2 (Figures 3A–3C).
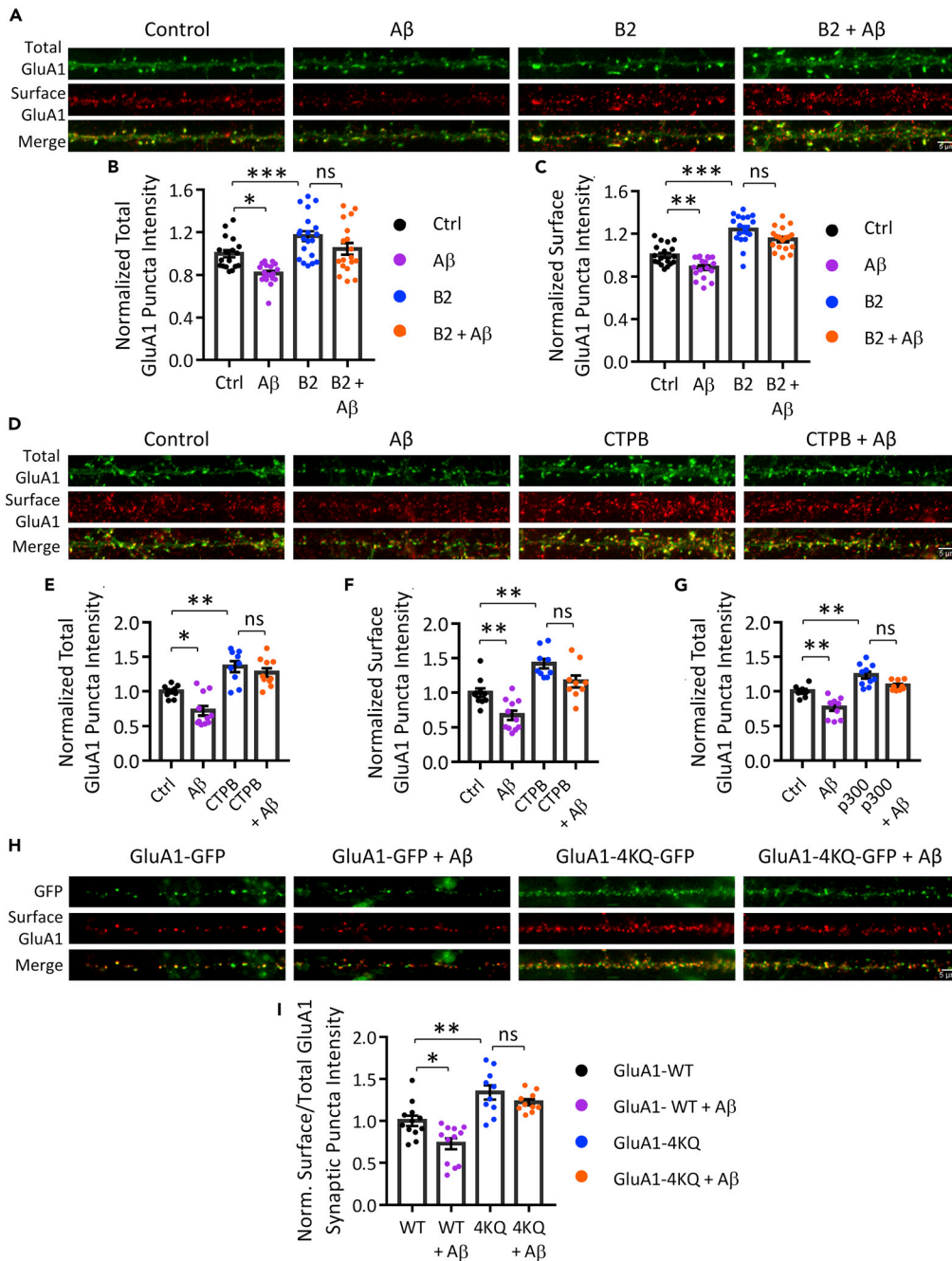
Figure 3. Acetylation Stabilizes AMPAR Synaptic Localization

(A) Cultured hippocampal neurons were treated with B2, to inhibit SIRT2 (Total GluA1, green; Surface GluA1, red) (scale bar, 5 μm).

(B–C) Quantification showed B2 treatment increased GluA1 puncta localization and blocked Aβ-induced reduction in GluA1 as measured by GluA1 (B) total and (C) surface puncta intensity (Ctrl, n = 17 cells, 21,486 puncta; Aβ, n = 19 cells, 25,742 puncta; B2, n = 17 cells, 14,838 puncta; B2 + Aβ, n = 17 cells, 11,524 puncta).

(D) CTPB treatment, to activate acetyltransferase activity of p300, followed by immunocytochemistry probing of GluA1 (Total GluA1, green; Surface GluA1, red) (scale bar, 5 μm).

(E–F) Quantification showed CTPB treatment increased GluA1 puncta localization and blocked Aβ-induced reduction in GluA1 puncta intensity as measured by GluA1 (E) total and (F) surface puncta intensity. (Ctrl, n = 10 cells, 2,615 puncta; Aβ, n = 11 cells, 3,964 puncta; CTPB, n = 8 cells, 4,383 puncta; CTPB + Aβ, n = 8 cells, 3,363 puncta).

Figure 3. *Continued*

(G) Overexpression of p300 increased total GluA1 puncta intensity and blocked Aβ-induced reduction (Ctrl, *n* = 7 cells, 336 puncta; Aβ, *n* = 10 cells, 332 puncta; p300, *n* = 10 cells, 337 puncta; p300 + Aβ, *n* = 9 cells, 351 puncta).

(H) Aβ treatment of hippocampal neurons overexpressing GluA1-WT-GFP or GluA1-4KQ-GFP acetylation mimetic (Surface GluA1, red) (scale bar, 5 μm).

(I) Quantitative analysis of surface expressing exogenous GluA1 normalized to total puncta expressing exogenous GluA1 showed GluA1-4KQ-GFP increased GluA1 surface expression and blocked Aβ-induced decrease in surface GluA1 levels (GluA1-WT, *n* = 8 cells, 798 puncta; GluA1-WT + Aβ, *n* = 9 cells, 943 puncta; GluA1-4KQ, *n* = 9 cells, 901 puncta; GluA1-4KQ + Aβ, *n* = 8 cells, 862 puncta).

*p<0.05, **p<0.01, ***p<0.001. Data are mean ± SEM.

To examine the role of acetyltransferase activity in Aβ-induced AMPAR reductions, DIV 15 hippocampal neurons were incubated with p300 acetyltransferase activator CTPB (20 μM), together with or without Aβ, for 24 h. We found that activation of p300 by CTPB resulted in an increase in total and surface GluA1 puncta (Figures 3D–3F). Similar to the effect of Sirt2 inhibition, activation of p300 resulted in a blockade of the Aβ-induced AMPAR reduction (Figures 3D–3F). To directly test the effect of the acetyltransferase, primary neurons were transfected with p300 at DIV 8, which were then incubated with Aβ at DIV14 for 24 h. Consistently, we found that, compared with control neurons expressing GFP, which showed a reduction in GluA1 by Aβ treatment, no changes were detected on GluA1 puncta intensity in neurons overexpressing p300 (Figure 3G).

GluA1 Acetylation Mimetic Confers AMPAR Resistance to the Aβ-Induced Down-Regulation

It has been shown that substitution of lysine with glutamine mimics constitutive acetylation as glutamine's hydrophilic and uncharged structure imitates that of an acetylated lysine (Kim et al., 2006). We therefore mutated the four lysine residues of GluA1 to glutamine (GluA1-4KQ) and used the construct as a GluA1 acetylation mimetic (Wang et al., 2017). We transfected DIV 8 hippocampal neurons with GFP-GluA1-WT or GFP-GluA1-4KQ and compared their expression after 1 week. Consistent with the effect of acetylation, we found that, compared with GFP-GluA1-WT, GFP-GluA1-4KQ retained significantly higher levels of surface expression relative to the total expressed at the synapse (Figures 3H and 3I). To determine whether this acetylation mimetic was also able to block the effect of Aβ on AMPAR levels, we treated GFP-GluA1-WT or GFP-GluA1-4KQ transfected DIV 14 neurons with Aβ for 24 h. Although Aβ incubation reduced the surface expression of GFP-GluA1-WT, the expression of acetyl-mimetic GFP-GluA1-4KQ was not changed in the presence of Aβ oligomers (Figures 3H and 3I). These results demonstrate that acetylated AMPARs become resistant to Aβ-induced down-regulation.

AMPAR Acetylation Suppresses Aβ-Induced Receptor Endocytosis

Our previous work and studies of others have shown that Aβ exposure causes AMPAR ubiquitination and internalization (Guntupalli et al., 2017; Miñano-Molina et al., 2011; Zhang et al., 2018). We wondered whether the acetylation of AMPARs also plays a role in the regulation of Aβ-induced internalization. To test this idea, we incubated DIV 14 hippocampal neurons with Aβ alone, or with CTPB, for 24 h and performed internalization assays. We found that CTPB treatment (20 μM) suppressed AMPAR internalization at basal conditions, indicated by a reduction of the ratio of internalized to surface GluA1 (Figures 4A and 4B). Furthermore, although treatment with Aβ alone (1 μM) resulted in an increase in AMPAR internalization as expected, co-incubation with CTPB abolished the Aβ effect on AMPAR trafficking (Figures 4A and 4B). It was possible that CTPB affected AMPAR trafficking via off-target effects of p300 activity. To directly determine the role of AMPAR acetylation in Aβ-induced receptor internalization, we examined receptor internalization using the GluA1 acetylation mimetic. DIV 8 cultured neurons were transfected with GFP-GluA1-WT or GFP-GluA1-4KQ, which were then treated with Aβ or vehicle control for 24 h before performing internalization assays on DIV 15. We found that the basal internalization of GFP-GluA1-4KQ was reduced compared with GFP-GluA1 (Figures 4C and 4D). Importantly, although Aβ treatment enhanced the internalization of GFP-GluA1, not significant effect was observed in cells expressing GFP-GluA1-4KQ (Figures 4C and 4D). These results indicate that modulation of AMPARs by direct acetylation causes suppression of both basal and Aβ-induced AMPAR internalization.

AMPARs Show Reduced Levels in Acetylation in APP/PS1 Mice

In AD, AMPARs have a facilitated turnover rate, leading to a reduction in the total amount and synaptic accumulation of AMPARs. As we found that acetylation was able to stabilize AMPARs and rescue the effect
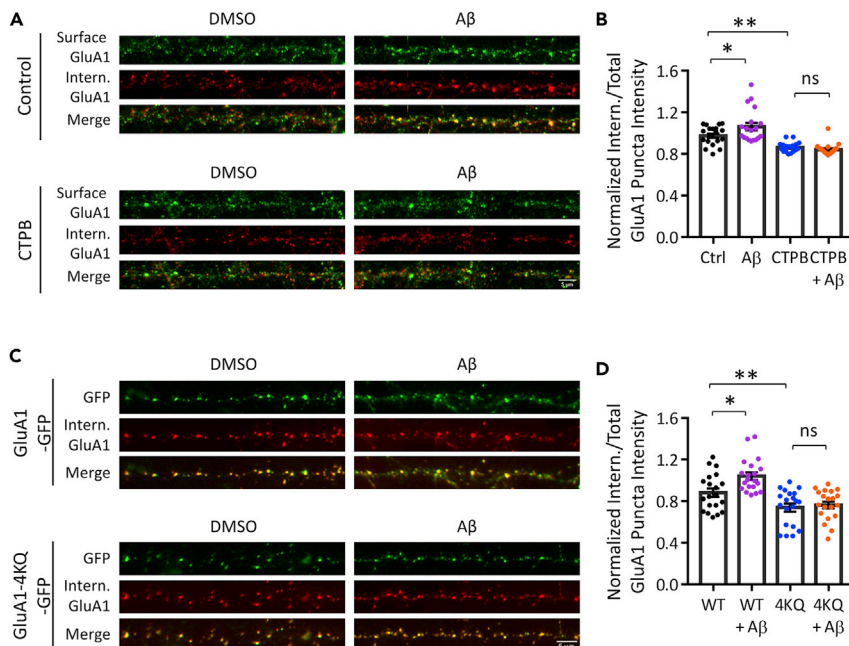
Figure 4. Acetylation Blocks Aβ-Induced Receptor Internalization

(A) Internalization assay of hippocampal neurons treated with CTPB, to activate acetyltransferase activity of p300, or CTPB with Aβ (Surface GluA1, green; Internalized GluA1, red) (scale bar, 5 μm).

(B) Quantification of the puncta intensity of internalized GluA1 to initial surface total GluA1 (internalized + remaining surface) showed CTPB treatment blocked Aβ-induced internalization of GluA1 (Ctrl, $n = 19$ cells, 2,095 puncta; Aβ, $n = 19$ cells, 2,124 puncta; CTPB, $n = 19$ cells, 6,230 puncta; CTPB + Aβ, $n = 19$ cells, 3,341 puncta).

(C) Internalization assay of hippocampal neurons overexpressing GluA1-WT or GluA1-4KQ with or without Aβ (Internalized GluA1, red) (scale bar, 5 μm).

(D) Quantitative analysis of the puncta intensity of internalized GluA1-GFP or GluA1-4KQ-GFP to total GluA1-GFP or GluA1-4KQ-GFP expressed at that puncta. Quantification showed Aβ-induced internalization of GluA1 is suppressed by overexpression of GluA1-4KQ (GluA1-WT, $n = 26$ cells, 2,637 puncta; GluA1-WT + Aβ, $n = 20$ cells, 2,161 puncta; GluA1-4KQ, $n = 20$ cells, 1,897 puncta; GluA1-4KQ + Aβ, $n = 20$ cells, 3,018 puncta).

*$p<0.5$, **$p<0.01$. Data are mean ± SEM.

of Aβ treatment *in vitro*, we wanted to know the role AMPAR acetylation plays *in vivo* and in AD conditions. As a widely used model of AD, the APP/PS1 mouse produces high levels of Aβ in the brain and demonstrates typical molecular and behavioral phenotypes of AD (McClean and Hölscher, 2014; Reinders et al., 2016; Reiserer et al., 2007; Sun et al., 2019; Trinchese et al., 2004). To determine whether AMPAR acetylation is altered in this AD animal model, we isolated GluA1 from hippocampal brain tissues of 11-month-old APP/PS1 mouse by immunoprecipitation and probed for acetylation and ubiquitination (Figure 5A). Indeed, consistent with our findings from rat primary neurons and human AD brains, this mouse model showed a significant reduction in the level of GluA1 acetylation, as well as an increase in GluA1 ubiquitination (Figures 5B and 5C). A reduction in GluA1 acetylation was also observed in APP/PS1 mice at 5 months old (Figure S2). The APP/PS1 mouse also showed significant reduction in the total amount of AMPARs, including GluA1 and GluA2, as well as the presynaptic proteins including synapsin I and synaptophysin, and the postsynaptic protein PSD95 (Figures 5F–5H). These changes in synaptic proteins are consistent with the known loss of synapses in the AD mouse (McClean and Hölscher, 2014; Shi et al., 2017).

Viral Expression of GluA1 and Its Acetylation Mimetic in APP/PS1 Mice

A reduction in AMPAR synaptic accumulation and the consequential suppression in synaptic strength is believed to be an early pathobiology in AD (Baglietto-Vargas et al., 2018; Hsieh et al., 2006; Kamenetz et al., 2003; Li et al., 2019; Lin et al., 2019; Sun et al., 2019; Ting et al., 2007). We therefore wanted to know whether stabilization of AMPARs by acetylation confers positive effects toward AD conditions. To examine the role of AMPAR acetylation for memory impairments in the AD animals, we injected AAV viruses expressing either GFP-GluA1-WT or GFP-GluA1-4KQ into the bilateral ventricles of
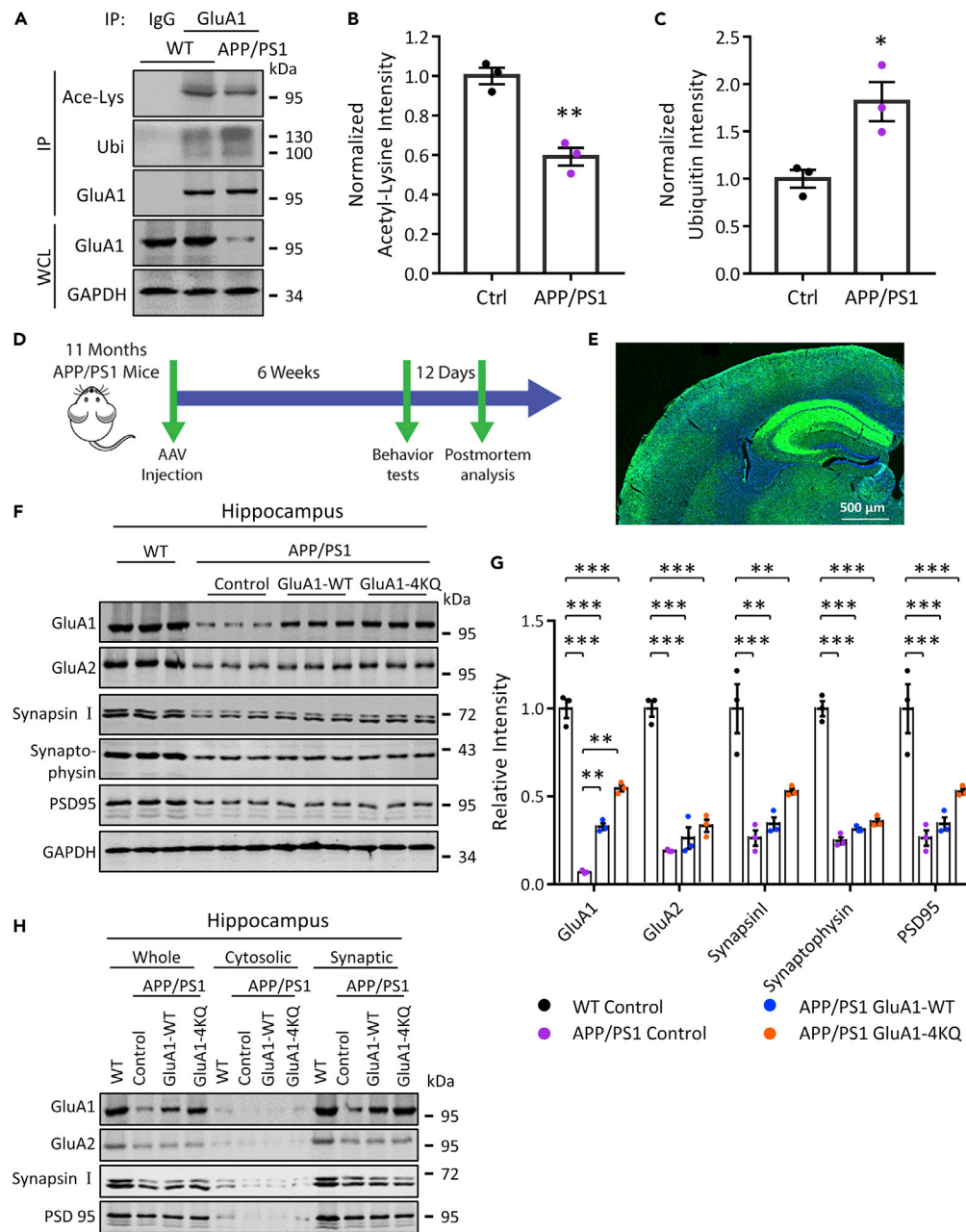
Figure 5. Viral Brain Injection of GluA1-4KQ Restores GluA1 Expression and Synaptic Accumulation and Rescues the Visual Episodic Memory Deficit in APP/PS1 Mice

(A) Hippocampal tissue from 11-month-old wild-type and APP/PS1 mouse brains was homogenized and immunoprecipitated with antibody against GluA1. GluA1 acetylation and ubiquitination levels were detected through probing the immunoprecipitated GluA1 with anti-Acetyl-Lysine or ubiquitin antibodies, respectively.

(B) Quantitative analysis of the GluA1 acetylation levels showed a reduction in AMPAR acetylation in APP/PS1 mice ($n = 3$ experiments).

(C) Quantification analysis of the GluA1 ubiquitination levels showed an increase in AMPAR ubiquitination in APP/PS1 mice ($n = 3$ experiments)

(D) Timeline of the experiment. AAV was injected into the bilateral ventricles of wild-type mice or APP/PS1 mice at 11 months.

(E) AAV expression was observed (green) 6 weeks after injection. Cell nuclei were stained with Hoechst (blue) to show the cortex and hippocampus (scale bar, 500 μm).

Figure 5. *Continued*

(F) GluA1, GluA2, synapsin I, synaptophysin, and PSD95 levels were detected by western blotting in mouse hippocampus. GAPDH was used as a loading control (*n* = 3 per group).

(G) Quantification shows a reduction in synaptic markers in APP/PS1 mouse brains with an increase in GluA1 from AAV injection of GluA1-WT or GluA1-4KQ.

(H) GluA1, GluA2, synapsin I, and PSD95 were detected by western blotting in whole-cell lysates, cytosolic fractions, and synaptosomal fractions of mouse hippocampus.

*p<0.05, **p<0.01, ***p<0.001. Data are mean $\pm$ SEM.

11-month-old APP/PS1 mice (Figure 5D). Another group of APP/PS1 mice were injected with a virus expressing only GFP as a control (APP/PS1-con). Six weeks after bilateral injection of the viruses, brain tissues were collected for examination. Brain slices revealed strong GFP signals, indicating efficient viral expression of the constructs (Figure 5E). Western blots of APP/PS1 hippocampal brain lysates showed a significant reduction in synaptic proteins including GluA1, GluA2, synapsin I, synaptophysin, and PSD95 (Figures 5F and 5G). Similar changes were observed in the cortex (Figures S1A and S1B). In APP/PS1 mice injected with either GFP-GluA1-WT or GFP-GluA1-4KQ, we found a specific increase in GluA1 in both the hippocampus (Figures 5F and 5G) and, to a lesser extent, in the cortex (Figures S1A and S1B) compared with APP/PS1 controls. Compared with GluA1-WT, GluA1-4KQ overexpression rescued GluA1 more significantly in APP/P1 mice (Figures 5H and S1C). It is noteworthy that GluA1 expression was preferentially increased in the synaptosomal fractions relative to the cytosolic fractions (Figures 5H and S1C). These results indicate the successful expression of the viral GluA1 and GluA1-4KQ AMPAR subunits at the synaptic sites of these brain regions.

Expression of GluA1 Acetylation Mimetic Rescues Deficits in Synaptic Plasticity in the APP/PS1 Mice

Synaptic plasticity serves as the molecular basis for learning and memory (Humeau and Choquet, 2019; Lüscher and Malenka, 2012; Nabavi et al., 2014; Parkinson and Hanley, 2018), which is known to be impaired in AD conditions (Colom-Cadena et al., 2020; Lambert et al., 1998; Li and Selkoe, 2020; Sánchez-Rodríguez et al., 2019; Shankar et al., 2008; Styr and Slutsky, 2018; Walsh et al., 2002). We wanted to know whether the improved synaptic expression of AMPARs by viral injection of GluA1-4KQ had any effect on synaptic function. Using hippocampal brain slices, we examined the expression of long-term potentiation (LTP) by recordings of field excitatory postsynaptic potentials (fEPSPs). Consistent with previous reports, recordings from APP/PS1 mice showed a significant reduction in LTP expression when compared with the wild-type mice (Gelman et al., 2018; Gengler et al., 2010; Da Silva et al., 2016; Trinchese et al., 2004; Vargas et al., 2014; Vyas et al., 2020) (Figures 6A and 6B). However, APP/PS1 mice expressing viral GFP-GluA1-4KQ had substantially improved LTP, whereas expression of GFP-GluA1-WT showed some rescue but to a lesser extent (Figures 6A and 6B). These results indicate that restoration of AMPAR stability and synaptic accumulation rescues synaptic plasticity.

Expression of GluA1 Acetylation Mimetic Rescues Visual Episodic Memory Deficits in APP/PS1 Mice

To examine the effect of GluA1 expression on cognitive function in the AD mice, we first performed the novel object recognition test to assess visual episodic memory in the virally injected APP/PS1 mice. Animals were first habituated to the apparatus by allowing them to explore the cage prior to the test. The animals were then allowed to familiarize themselves with the initial objects A and B. The preference index from the familiarization period showed a lack of preference for either of the objects (data not shown). After 1 and 24 h, animals were brought back to the cage with object B being replaced with object C and then object D (Figure 6C). As measured by the discrimination index, APP/PS1 mice struggled to remember the familiar object and thus failed to discriminate between the objects (Figure 6D). In the familiarization stage, none of the animals showed a particular preference of either of the objects (Figure 6E). During the 1 and 24 h tests, APP/PS1 mice spent similar amounts of time with familiar object A and either of the novel objects C or D, respectively, indicating impairments in short-term and long-term memory (Figures 6F and 6G). APP/PS1 mice expressing viral GluA1 spent significantly more time with the novel object compared with the familiar object in both the 1 and 24 h tests (Figures 6F and 6G). Viral expression of GluA1-WT led to modest improvements in memory, whereas more robust rescue effects were observed in animals expressing the acetylation mimetic GluA1-4KQ, at both 1 and 24 h after training (Figure 6D). These findings
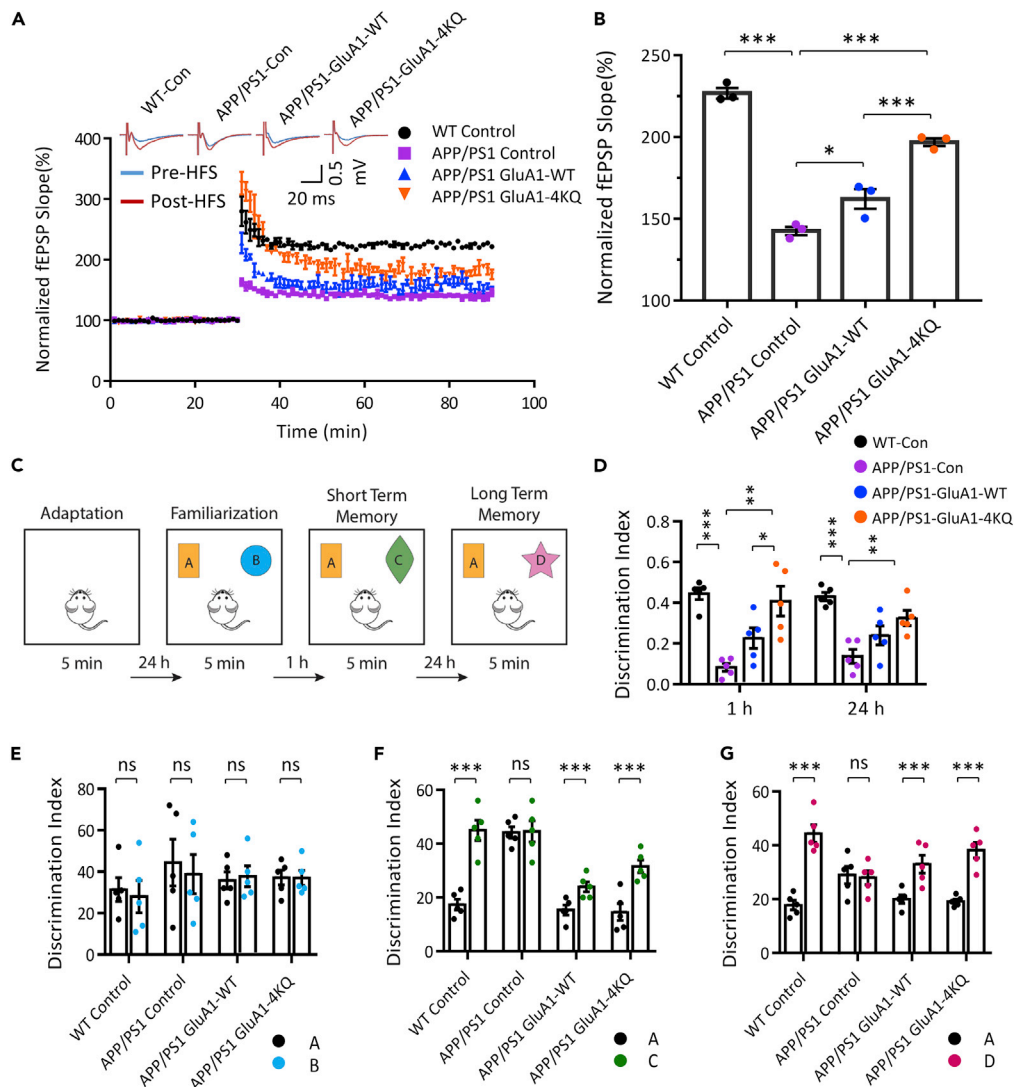
Figure 6. Overexpression of GluA1-4KQ Rescues Hippocampal LTP and the Visual Episodic Memory Deficit in APP/PS1 Mice

(A) LTP recordings of fEPSP in acute hippocampal slices from AAV-injected wild-type mice or APP/PS1 mice.

(B) Quantitative analysis of the normalized fEPSP slope ($n = 2$ animals per condition, 3 brain slices per animal).

(C) The experimental design of novel object recognition test (NOR). One day before the memory acquisition, the mice were habituated to the arenas for 5 min, as indicated in the first box. The second box showed the acquisition trial. The third and fourth boxes showed the test trial conducted 1 and 24 h after the acquisition trial.

(D) The discrimination index of 1 and 24 h test trials.

(E) The recognition index between objects A and B in the acquisition trial.

(F) The recognition index between objects A and C in the test trial 1 h after the acquisition trial.

(G) The recognition index between objects A and D in the test trial 24 h after the acquisition trial ($n = 5$ animals).

*$p<0.05$, **$p<0.01$, ***$p<0.001$. Data are mean $\pm$ SEM.

indicate that addition of acetylated, and thus stabilized, AMPARs is capable of correcting the impairments in memory capacity in AD mice.

GluA1 Acetylation Mimetic in APP/PS1 Mice Rescues Spatial Memory

We next sought to investigate the role of AMPAR acetylation in spatial learning and memory by the Morris water maze. In this test, mice were trained over a period of 4 days to learn the location of an escape
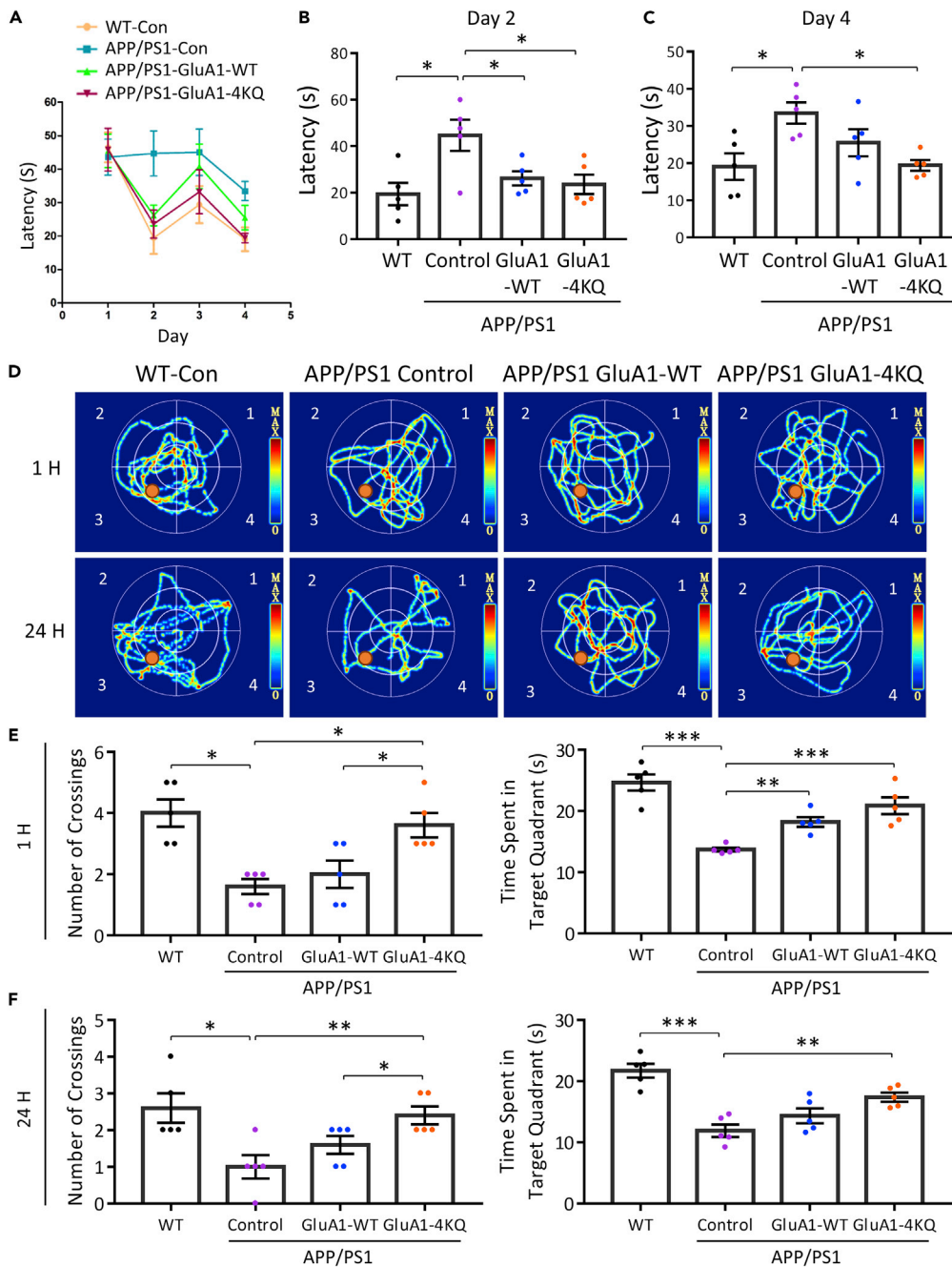
Figure 7. Overexpression of GluA1-4KQ Rescues the Spatial Learning and Memory Deficit in APP/PS1 Mice

(A) The latency to reach the hidden platform during training in Morris Water Maze.

(B) The latency of day 2 of the training.

(C) The latency of day 4 of the training.

(D) The representative searching trace after removing the platform in the probe trial at 1 and 24 h after training.

(E) Left: The number of crosses over the platform site after removing the platform (1 h) during the probe trial. Right: The percentage of time spent in target quadrant.

(F) Left: The number of crosses over the platform site after removing the platform (24 h) during the probe trial. Right: The percentage of time spent in target quadrant (*n* = 5 animals).

*p<0.05, **p<0.01, ***p<0.001. Data are mean ± SEM.

platform in a pool of water using spatial cues placed within the testing room. On the second day of training, the control APP/PS1 mice had difficulties in finding the platform, whereas mice with GluA1-4KQ or GluA1 virus were able to find the platform as fast as WT mice (Figures 7A and 7B). The difference in performance was maintained for a substantial amount of time; at the end of training on day 4, mice expressing GluA1-4KQ still performed significantly better than those expressing viral GFP (Figure 7C).

At 1 and 24 h after spatial acquisition training, animals were placed back in the pool with the escape platform removed to test spatial memory (Figure 7D). Animals with intact memory can remember the location of the escape platform from training and are expected to spend time exploring the area where the platform was previously located. We analyzed the number of events when animals swam across the platform's former location, as well as the time spent in the target quadrant of the pool. In the 1 h post-training test, GluA1-4KQ expressing animals made significantly more crossings over the target location and had a significant increase in the time spent in the target quadrant, compared with APP/PS1 control animals (Figure 7E). Probing of spatial memory 24 h after training showed that GluA1-4KQ-expressing animals maintained a significant improvement in the number of crossings and time spent in the target quadrant compared with APP/ PS1 mice (Figure 7F). These findings indicate that expression of GluA1-4KQ is capable of rescuing the impairments in spatial memory observed in APP/PS1 mice.

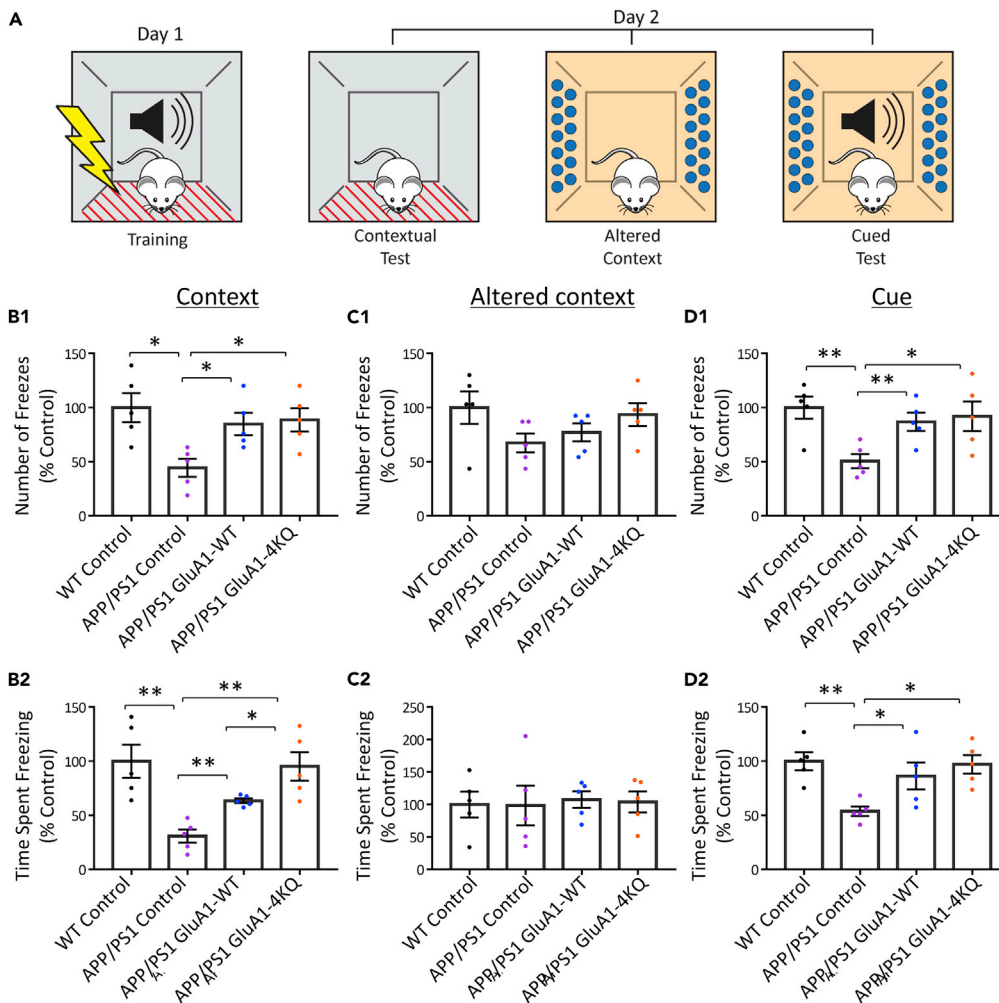### GluA1 Acetylation Mimetic in APP/PS1 Mice Rescues Fear Memory

To further examine the role of AMPAR acetylation in memory, we next performed a fear conditioning test. On day 1, mice were placed into the fear conditioning chamber and subjected to a stimulation protocol with a 2-s foot shock paired with a 20-s tone to condition a fear response. After 24 h the animals were placed back into the same box under the same environmental conditions, and the contextual memory was assessed by quantifying the amount of time spent freezing and the number of freezing instances. One hour after the contextual memory text, the entire environment of the box was changed, including both odorants and wall and floor materials/design. One hour after exposure to this new context, the cued memory was measured by quantifying the amount of freezing time and number of freezes made after the conditioned tone was played (Figure 8A).

In the contextual memory test, APP/PS1 mice showed a significant impairment in hippocampal-based, contextual fear memory compared with WT animals, with a decrease in both the number of freezing instances and total freezing time (Figure 8B). However, the APP/PS1 mice expressing GluA1-4KQ froze a significantly greater number of times (Figure 8B1) and for a greater length of time than the APP/PS1 mice (Figure 8B2), indicating improved memory of the testing chamber. In the test of cue memory, all of the animal groups showed a minimal freezing behavior in the testing chamber with an altered context, indicating no fear had been associated with this new environment (Figure 8C). However, when the tone was played, WT animals demonstrated strong cued fear memory, showing an elevation in freezing behavior, whereas APP/PS1 animals did not (Figure 8D). In contrast, APP/PS1 animals expressing GluA1-4KQ showed an increased number of freezes (Figure 8D1) and prolonged total freezing time (Figure 8D2), comparable with the level of WT animals. These results indicate that the impairments in both contextual and cued fear memory were rescued by the introduction of GluA1-4KQ in APP/PS1 mice.

In most behavior tests in our study, besides significant rescue effect when compared with APP/PS1 mice, GluA1-4KQ-overexpressing APP/PS1 mice showed a better performance than GluA1-WT-overexpressing APP/PS1 mice, indicating that GluA1-4KQ is more effective in preventing learning and memory impairments in AD animal model.

DISCUSSION

One of the earliest pathological features of AD is an impairment in synaptic function partly due to a reduction in AMPA receptors at the synapse (Almeida et al., 2005; Baglietto-Vargas et al., 2018; Chang et al., 2006; Dong et al., 2015; Li et al., 2019; Marttinen et al., 2018). It has been shown that soluble Aβ oligomers promote AMPAR internalization and degradation (Guntupalli et al., 2017; Miñano-Molina et al., 2011). This is consistent with studies of our own, and those of others, which show an increase in ubiquitination of AMPARs in AD (Guntupalli et al., 2017; Rodrigues et al., 2016; Zhang et al., 2018) (as reviewed by Harris et al., 2020; Moraes et al., 2020; Zhu and Tsai, 2020). Findings from our recent work have revealed for the first time that AMPARs are also subject to acetylation, a new form of AMPAR regulation that antagonizes receptor ubiquitination due to competition for the same lysine residues (Wang et al., 2017). In this study, we further

Figure 8. Overexpression of GluA1-4KQ Rescues Fear Memory Deficits in APP/PS1 Mice

(A) The schematic diagram of the experimental design.

(B) The total number of freezes (B1) and total time spent freezing (B2) were detected in the contextual fear conditioning test.

(C) The total number of freezes (C1) and total time spent freezing (C2) were detected in the altered contextual fear conditioning test.

(D) The total number of freezes (D1) and total time spent freezing (D2) were detected in the tone-dependent freezing behavior test (n = 5 animals).

*$p<0.05$, **$p<0.01$. Data are mean $\pm$ SEM.

investigated the molecular mechanism involved in AMPAR acetylation and examined the role of AMPAR acetylation in cognitive deficits in AD.

We found that, in brain lysates from patients with AD, a reduction in total AMPAR amount is accompanied with a decrease in acetylation of AMPARs. The change in AMPAR acetylation was also observed in the brains of APP/PS1 AD mice. Consistently, treatment of neuronal cultures with soluble Aβ oligomers led to a significant reduction in the level of AMPAR acetylation.

In our previous work, SIRT2 was identified as the deacetylase for AMPAR deacetylation (Wang et al., 2017); however, the related acetyltransferase remained unknown. In this study, we discovered that p300 functions as the acetyltransferase responsible for AMPAR acetylation. Although p300 is generally known for its role in acetylation of nuclear histone proteins, it also localizes in the cytosol where it acetylates various substrates (Aslan et al., 2015; Dancy and Cole, 2015; Kwok et al., 2006; Rotte et al., 2013; Sebti et al., 2014; Shi et al.,

2009). Our results demonstrate that p300 acetyltransferase activity triggers acetylation of AMPARs, resulting in a reduced rate in receptor internalization and degradation, leading to an increase in AMPAR cell-surface expression and elevated accumulation at the synapse.

The implication of AMPAR acetylation in brain function may vary depending on the basal levels of AMPAR protein amount and the extent of AMPAR acetylation. In this study, an increase in AMPAR acetylation led to improvements in memory in the APP/PS1 AD mice. Under AD conditions, a dramatic reduction in overall AMPAR amount is a major factor in causing synaptic weakening and impairments in cognition. Therefore, reintroduction of the acetylated and stabilized AMPARs restores the level of AMPARs and synaptic activity, leading to rescue of AD-related memory deficits. Interestingly, over-stabilization of AMPARs via enhanced receptor acetylation seems to have different effect on brain function. Indeed, wild-type mice expressing the stabilized acetylation mimetic GluA1, as well as knockout mice lacking the deacetylase SIRT2, showed impairments in synaptic plasticity and memory (Wang et al., 2017). This memory impairment likely results from excessive over-stabilization of acetylated AMPARs at synapses. In normal non-AD animals, a dramatic increase in AMPAR acetylation disrupts receptor trafficking and turnover, which is probably the cause for synaptic dysregulation and memory deficits (Wang et al., 2017).

Given their crucial role in interneuronal communication and brain function, AMPARs have been identified as a therapeutic target for several neurological disorders (Hettinger et al., 2018; Lee et al., 2016; Lynch, 2006; Paula-Lima et al., 2013; Swanson, 2009; Zhang et al., 2019). Our findings provide further support for potential strategies targeting AMPARs for the treatment of AD-related cognitive dysfunctions. Thus far, the main treatment focus has been the use of positive allosteric modulators of AMPAR known as Ampakines (Bernard et al., 2010; Black, 2005; Fernandes et al., 2018; Ward et al., 2010), a few of which have gone to clinical trial. However, although compounds showed some success in animal models (Bretin et al., 2017; Giralt et al., 2017; Lauterborn et al., 2016), they have had low clinical success (Bernard et al., 2019; Trzepacz et al., 2013; Wezenberg et al., 2007). Owing to a lack of chemical diversity among the Ampakines, alternative strategies for AMPAR-based treatment are being considered (Chang et al., 2012; Hao et al., 2015; Lee et al., 2016; Zhao et al., 2019). Our results provide a basis for pharmacological manipulation of AMPAR acetylation as a potential therapeutic strategy. On a broader level, because ubiquitination, a modulation antagonizing acetylation and resulting in receptor degradation, is enhanced in AD (Gadhave et al., 2016; Liu et al., 2019; Tramutola et al., 2018), manipulation of both of these opposing processes should be considered for more efficient management of AD.

In conclusion, our results show that the acetylation of AMPARs leads to a blockage of Aβ-induced reduction of AMPARs at the synapse by preventing receptor internalization, resulting in significant improvements in learning and memory in the transgenic AD mice. These findings encourage future efforts to identify novel compounds that enhance AMPAR acetylation as potential therapeutic tools for patients with AD.

Limitations of the Study

In APP/PS1 mice, GluA1 acetylation mimetic GluA1-4KQ was introduced by viral expression, the effect of endogenous AMPAR acetylation will be explored in future studies by overexpressing the acetyltransferase p300, or by application of its enzyme activators. Also, the findings were based on primary neurons and an AD mouse model; thus, their value for translational medicine in humans remains unclear.

Resource Availability

Lead Contact

Further information and requests for resources should be directed to and will be fulfilled by the Lead Contact, Dr. Hengye Man (hman@bu.edu; rong.liu@hust.edu.cn).

Materials Availability

This study did not generate new unique reagents.

Data and Code Availability

This study did not generate datasets or code.

AUTHOR CONTRIBUTIONS

This study was directed and supervised by H.-Y.M. and R.L. M.O. and Y.-P.S. performed most of the experiments and the data analysis. G.W. performed some acetylation westerns. W.-T.H. participated in animal behavior tests. W.-T.H., Z.-D.X., and X.-C.W provided some APP/PS1 AD mouse brain tissue and some reagents. M.O. and H.-Y.M. wrote the manuscript. R.L. and Y.-P.S. assisted in manuscript preparation.

DECLARATION OF INTERESTS

The authors declare that there is no potential conflict of interest.

REFERENCES

Alaei, S.R., Abrams, C.K., Bulinski, J.C., Hertzberg, E.L., and Freidin, M.M. (2018). Acetylation of C-terminal lysines modulates protein turnover and stability of Connexin-32. BMC Cell Biol. 19, 22.

Alfonso, S., Kessels, H.W., Banos, C.C., Chan, T.R., Lin, E.T., Kumaravel, G., Scannevin, R.H., Rhodes, K.J., Huganir, R., Guckian, K.M., et al. (2014). Synapto-depressive effects of amyloid beta require PICK1. Eur. J. Neurosci. 39, 1225–1233.

Almeida, C.G., Tampellini, D., Takahashi, R.H., Greengard, P., Lin, M.T., Snyder, E.M., and Gouras, G.K. (2005). Beta-amyloid accumulation in APP mutant neurons reduces PSD-95 and GluR1 in synapses. Neurobiol. Dis. 20, 187–198.

Armstrong, D.M., Ikonomovic, M.D., Sheffield, R., and Wenthold, R.J. (1994). AMPA-selective glutamate receptor subtype immunoreactivity in the entorhinal cortex of non-demented elderly and patients with Alzheimer's disease. Brain Res. 639, 207–216.

Aslan, J.E., Rigg, R.A., Nowak, M.S., Loren, C.P., Baker-Groberg, S.M., Pang, J., David, L.L., and Mccarty, O.J.T. (2015). Lysine acetyltransfer supports platelet function. J. Thromb. Haemost. 13, 1908–1917.

Baglietto-Vargas, D., Prieto, G.A., Limon, A., Forner, S., Rodriguez-Ortiz, C.J., Ikemura, K., Ager, R.R., Medeiros, R., Trujillo-Estrada, L., Martini, A.C., et al. (2018). Impaired AMPA signaling and cytoskeletal alterations induce early synaptic dysfunction in a mouse model of Alzheimer's disease. Aging Cell 17, e12791.

Balasubramanyam, K., Swaminathan, V., Ranganathan, A., and Kundu, T.K. (2003). Small molecule modulators of histone acetyltransferase p300. J. Biol. Chem. 278, 19134–19140.

Bernard, K., Danober, L., Thomas, J.-Y., Lebrun, C., Muñoz, C., Cordi, A., Desos, P., Lestage, P., and Morain, P. (2010). Drug focus: S 18986: a positive allosteric modulator of AMPA-type glutamate receptors pharmacological profile of a novel cognitive enhancer. CNS Neurosci. Ther. 16, e193–e212.

Bernard, K., Gouttefangeas, S., Bretin, S., Galtier, S., Robert, P., Holthoff-Detto, V., Cummings, J., and Pueyo, M. (2019). A 24-week double-blind placebo-controlled study of the efficacy and safety of the AMPA modulator S47445 in patients with mild to moderate Alzheimer's disease and depressive symptoms. Alzheimer's Dement. Transl. Res. Clin. Interv. 5, 231–240.

Black, M.D. (2005). Therapeutic potential of positive AMPA modulators and their relationship to AMPA receptor subunits. A review of preclinical data. Psychopharmacology (Berl) 179, 154–163.

Bowers, E.M., Yan, G., Mukherjee, C., Orry, A., Wang, L., Holbert, M.A., Crump, N.T., Hazzalin, C.A., Liszczak, G., Yuan, H., et al. (2010). Virtual ligand screening of the p300/CBP histone acetyltransferase: identification of a selective small molecule inhibitor. Chem. Biol. 17, 471–482.

Bretin, S., Louis, C., Seguin, L., Wagner, S., Thomas, J.-Y., Challal, S., Rogez, N., Albinet, K., Iop, F., Villain, N., et al. (2017). Pharmacological

characterisation of S 47445, a novel positive allosteric modulator of AMPA receptors. PLoS One 12, e0184429.

Cantanelli, P., Sperduti, S., Ciavardelli, D., Stuppia, L., Gatta, V., and Sensi, S.L. (2014). Age-dependent modifications of AMPA receptor subunit expression levels and related cognitive effects in 3xTg-AD mice. Front. Aging Neurosci. 6, 200.

Caron, C., Boyault, C., and Khochbin, S. (2005). Regulatory cross-talk between lysine acetylation and ubiquitination: role in the control of protein stability. Bioessays 27, 408–415.

Carter, T.L., Rissman, R.A., Mishizen-Eberz, A.J., Wolfe, B.B., Hamilton, R.L., Gandy, S., and Armstrong, D.M. (2004). Differential preservation of AMPA receptor subunits in the hippocampi of Alzheimer's disease patients according to Braak stage. Exp. Neurol. 187, 299–309.

Chang, E.H., Savage, M.J., Flood, D.G., Thomas, J.M., Levy, R.B., Mahadomrongkul, V., Shirao, T., Aoki, C., and Huerta, P.T. (2006). AMPA receptor downscaling at the onset of Alzheimer's disease pathology in double knockin mice. Proc. Natl. Acad. Sci. U S A 103, 3410–3415.

Chang, P.K.-Y., Verbich, D., and McKinney, R.A. (2012). AMPA receptors as drug targets in neurological disease - advantages, caveats, and future outlook. Eur. J. Neurosci. 35, 1908–1916.

Chen, Q.-S., Kagan, B.L., Hirakura, Y., and Xie, C.-W. (2000). Impairment of hippocampal long-term potentiation by Alzheimer amyloid β-peptides. J. Neurosci. Res. 60, 65–72.

Chidambaram, S.B., Rathipriya, A.G., Bolla, S.R., Bhat, A., Ray, B., Mahalakshmi, A.M., Manivasagam, T., Thenmozhi, A.J., Essa, M.M., Guillemin, G.J., et al. (2019). Dendritic spines: revisiting the physiological role. Prog. Neuropsychopharmacol. Biol. Psychiatry 92, 161–193.

Collingridge, G.L., Isaac, J.T.R., and Wang, Y.T. (2004). Receptor trafficking and synaptic plasticity. Nat. Rev. Neurosci. 5, 952–962.

Colom-Cadena, M., Spires-Jones, T., Zetterberg, H., Blennow, K., Caggiano, A., Dekosky, S.T., Fillit, H., Harrison, J.E., Schneider, L.S., Scheltens, P., et al. (2020). The clinical promise of biomarkers of synapse damage or loss in Alzheimer's disease. Alzheimers Res. Ther. 12, 1–12.

D'Amelio, M., Cavallucci, V., Middei, S., Marchetti, C., Pacioni, S., Ferri, A., Diamantini, A., De Zio, D., Carrara, P., Battistini, L., et al. (2011). Caspase-3 triggers early synaptic dysfunction in a mouse model of Alzheimer's disease. Nat. Neurosci. 14, 69–79.

Dancy, B.M., and Cole, P.A. (2015). Protein lysine acetylation by p300/CBP. Chem. Rev. 115, 2419–2452.

Derkach, V.A., Oh, M.C., Guire, E.S., and Soderling, T.R. (2007). Regulatory mechanisms of AMPA receptors in synaptic plasticity. Nat. Rev. Neurosci. 8, 101–113.

Dewar, D., Chalmers, D.T.T., Graham, D.I.I., and McCulloch, J. (1991). Glutamate Metabotropic and AMPA Binding Sites Are Reduced in Alzheimer's Disease: An Autoradiographic Study of the hippocampus (Elsevier).

Dong, Z., Han, H., Li, H., Bai, Y., Wang, W., Tu, M., Peng, Y., Zhou, L., He, W., Wu, X., et al. (2015). Long-term potentiation decay and memory loss are mediated by AMPAR endocytosis. J. Clin. Invest. 125, 234–247.

Drazic, A., Myklebust, L.M., Ree, R., and Arnesen, T. (2016). The world of protein acetylation. Biochim. Biophys. Acta 1864, 1372–1401.

Du, Y., Fu, M., Huang, Z., Tian, X., Li, J., Pang, Y., Song, W., Tian Wang, Y., and Dong, Z. (2020). TRPV1 activation alleviates cognitive and synaptic plasticity impairments through inhibiting AMPAR endocytosis in APP23/PS45 mouse model of Alzheimer's disease. Aging Cell 19, e13113.

Fernandes, D., Silva, J., Sotiropoulos, I., and Bretin, S. (2018). A novel modulator of AMPA receptors against Alzheimer's Disease pathology: the first in vivo evidence. Eur. Neuropsychopharmacol. 28, S56–S57.

Forner, S., Martini, A.C., Prieto, G.A., Dang, C.T., Rodriguez-Ortiz, C.J., Reyes-Ruiz, J.M., Trujillo-Estrada, L., da Cunha, C., Andrews, E.J., Phan, J., et al. (2019). Intra- and extracellular β-amyloid overexpression via adeno-associated virus-mediated gene transfer impairs memory and synaptic plasticity in the hippocampus. Sci. Rep. 9, 1–11.

Gadhave, K., Bolshette, N., Ahire, A., Pardeshi, R., Thakur, K., Trandafir, C., Istrate, A., Ahmed, S., Lahkar, M., Muresanu, D.F., et al. (2016). The ubiquitin proteasomal system: a potential target for the management of Alzheimer's disease. J. Cell. Mol. Med. 20, 1392–1407.

Gao, L., Tian, M., Zhao, H.-Y., Xu, Q.-Q., Huang, Y.-M., Si, Q.-C., Tian, Q., Wu, Q.-M., Hu, X.-M., Sun, L.-B., et al. (2016). TrkB activation by 7, 8-dihydroxyflavone increases synapse AMPA subunits and ameliorates spatial memory deficits in a mouse model of Alzheimer's disease. J. Neurochem. 136, 620–636.

Gelman, S., Palma, J., Tombaugh, G., and Ghavami, A. (2018). Differences in synaptic dysfunction between rTg4510 and APP/PS1 mouse models of Alzheimer's disease. J. Alzheimers Dis. 61, 195–208.

Gengler, S., Hamilton, A., and Hölscher, C. (2010). Synaptic plasticity in the Hippocampus of a APP/PS1 mouse model of Alzheimer's disease is impaired in old but not young mice. PLoS One 5, e9764.

Giralt, A., Gómez-Climent, M.Á., Alcalá, R., Bretin, S., Bertrand, D., María Delgado-García, J., Pérez-Navarro, E., Alberch, J., and Gruart, A. (2017). The AMPA receptor positive allosteric modulator S 47445 rescues in vivo CA3-CA1 long-term potentiation and structural synaptic changes in old mice. Neuropharmacology 123, 395–409.

Gong, Y., Lippa, C.F., Zhu, J., Lin, Q., and Rosso, A.L. (2009). Disruption of glutamate receptors at Shank-postsynaptic platform in Alzheimer's disease. Brain Res. 1292, 191–198.

Goo, M.S., Scudder, S.L., and Patrick, G.N. (2015). Ubiquitin-dependent trafficking and turnover of ionotropic glutamate receptors. Front. Mol. Neurosci. 8, 60.

Gu, Z., Liu, W., and Yan, Z. (2009). B-amyloid impairs AMPA receptor trafficking and function by reducing Ca2+/calmodulin-dependent protein kinase II synaptic distribution. J. Biol. Chem. 284, 10639–10649.

Guntupalli, S., Widagdo, J., and Anggono, V. (2016). Amyloid- β -induced dysregulation of AMPA receptor trafficking. Neural Plast. 2016, 1–12.

Guntupalli, S., Jang, S.E., Zhu, T., Huganir, R.L., Widagdo, J., and Anggono, V. (2017). GluA1 subunit ubiquitination mediates amyloid-β-induced loss of surface α-amino-3-hydroxy-5-methyl-4-isoxazolepropionic acid (AMPA) receptors. J. Biol. Chem. 292, 8186–8194.

Hao, J.-R., Sun, N., Lei, L., Li, X.-Y., Yao, B., Sun, K., Hu, R., Zhang, X., Shi, X.-D., and Gao, C. (2015). L-Stepholidine rescues memory deficit and synaptic plasticity in models of Alzheimer's disease via activating dopamine D1 receptor/PKA signaling pathway. Cell Death Dis. 6, e1965.

Harris, L.D., Jasem, S., and Licchesi, J.D.F. (2020). The ubiquitin system in Alzheimer's disease. In Advances in Experimental Medicine and Biology, R. Barrio, J. Sutherland, and M. Rodriguez, eds. (Springer), pp. 195–221.

Hettinger, J.C., Lee, H., Bu, G., Holtzman, D.M., and Cirrito, J.R. (2018). AMPA-ergic regulation of amyloid-β levels in an Alzheimer's disease mouse model. Mol. Neurodegener. 13, 22.

Hou, Q., Gilbert, J., and Man, H.Y. (2011). Homeostatic regulation of AMPA receptor trafficking and degradation by light-controlled single-synaptic activation. Neuron 72, 806–818.

Hsieh, H., Boehm, J., Sato, C., Iwatsubo, T., Tomita, T., Sisodia, S., and Malinow, R. (2006). AMPAR removal underlies Aβ-induced synaptic depression and dendritic spine loss. Neuron 52, 831–843.

Humeau, Y., and Choquet, D. (2019). The next generation of approaches to investigate the link between synaptic plasticity and learning. Nat. Neurosci. 22, 1536–1543.

Huo, Y., Khatri, N., Hou, Q., Gilbert, J., Wang, G., and Man, H.-Y. (2015). The deubiquitinating enzyme USP46 regulates AMPA receptor ubiquitination and trafficking. J. Neurochem. 134, 1067–1080.

Inuzuka, H., Gao, D., Finley, L.W.S., Yang, W., Wan, L., Fukushima, H., Chin, Y.R., Zhai, B., Shaik, S., Lau, A.W., et al. (2012). Acetylation-dependent regulation of Skp2 function. Cell 150, 179–193.

Jacob, C.P., Koutsilieri, E., Bartl, J., Neuen-Jacob, E., Arzberger, T., Zander, N., Ravid, R., Roggendorf, W., Riederer, P., and Grünblatt, E. (2007). Alterations in expression of glutamatergic transporters and receptors in sporadic Alzheimer's disease. J. Alzheimers Dis. 11, 97–116.

Jarzylo, L.A., and Man, H.Y. (2012). Parasynaptic NMDA receptor signaling couples neuronal glutamate transporter function to AMPA receptor synaptic distribution and stability. J. Neurosci. 32, 2552–2563.

Ju, J., and Zhou, Q. (2018). Dendritic spine modifications in brain physiology. In Neuroplasticity - Insights of Neural Reorganization (InTech).

Kamenetz, F., Tomita, T., Hsieh, H., Seabrook, G., Borchelt, D., Iwatsubo, T., Sisodia, S., and Malinow, R. (2003). APP processing and synaptic function. Neuron 37, 925–937.

Kim, M.Y., Woo, E.M., Chong, Y.T.E., Homenko, D.R., and Kraus, W.L. (2006). Acetylation of estrogen receptor alpha by p300 at lysines 266 and 268 enhances the deoxyribonucleic acid binding and transactivation activities of the receptor. Mol. Endocrinol. 20, 1479–1493.

Kopec, C.D., Li, B., Wei, W., Boehm, J., and Malinow, R. (2006). Glutamate receptor exocytosis and spine enlargement during chemically induced long-term potentiation. J. Neurosci. 26, 2000–2009.

Kwok, R.P.S., Liu, X.-T., and Smith, G.D. (2006). Distribution of co-activators CBP and p300 during mouse oocyte and embryo development. Mol. Reprod. Dev. 73, 885–894.

Lambert, M.P., Barlow, A.K., Chromy, B.A., Edwards, C., Freed, R., Liosatos, M., Morgan, T.E., Rozovsky, I., Trommer, B., Viola, K.L., et al. (1998). Diffusible, nonfibrillar ligands derived from Aβ1-42 are potent central nervous system neurotoxins. Proc. Natl. Acad. Sci. U S A 95, 6448–6453.

Lauterborn, J.C., Palmer, L.C., Jia, Y., Pham, D.T., Hou, B., Wang, W., Trieu, B.H., Cox, C.D., Kantorovich, S., Gall, C.M., et al. (2016). Chronic ampakine treatments stimulate dendritic growth and promote learning in middle-aged rats. J. Neurosci. 36, 1636–1646.

Lee, K., Goodman, L., Fourie, C., Schenk, S., Leitch, B., and Montgomery, J.M. (2016). AMPA

receptors as therapeutic targets for neurological disorders. Adv. Protein Chem. Struct. Biol. 103, 203–261.

Li, S., and Selkoe, D.J. (2020). A mechanistic hypothesis for the impairment of synaptic plasticity by soluble Aβ oligomers from Alzheimer's brain. J. Neurochem. 1–15.

Li, N., Li, Y., Li, L.-J., Zhu, K., Zheng, Y., and Wang, X.-M. (2019). Glutamate receptor delocalization in postsynaptic membrane and reduced hippocampal synaptic plasticity in the early stage of Alzheimer's disease. Neural Regen. Res. 14, 1037.

Li, S., Jin, M., Koeglsperger, T., Shepardson, N.E., Shankar, G.M., and Selkoe, D.J. (2011). Soluble Aβ oligomers inhibit long-term potentiation through a mechanism involving excessive activation of extrasynaptic NR2B-containing NMDA receptors. J. Neurosci. 31, 6627–6638.

Lin, A., Hou, Q., Jarzylo, L., Amato, S., Gilbert, J., Shang, F., and Man, H.-Y. (2011). Nedd4-mediated AMPA receptor ubiquitination regulates receptor turnover and trafficking. J. Neurochem. 119, 27–39.

Lin, L., Liu, A., Li, H., Feng, J., and Yan, Z. (2019). Inhibition of histone methyltransferases EHMT1/2 reverses amyloid-β-induced loss of AMPAR currents in human stem cell-derived cortical neurons. J. Alzheimers Dis. 70, 1175–1185.

Liu, X., Hebron, M.L., Mulki, S., Wang, C., Lekah, E., Ferrante, D., Shi, W., Kurd-Misto, B., and Moussa, C. (2019). Ubiquitin specific protease 13 regulates tau accumulation and clearance in models of Alzheimer's disease. J. Alzheimers Dis. 72, 425–441.

Lledo, P.M., Zhang, X., Südhof, T.C., Malenka, R.C., and Nicoll, R.A. (1998). Postsynaptic membrane fusion and long-term potentiation. Science 279, 399–403.

Lüscher, C., and Malenka, R.C. (2012). NMDA receptor-dependent long-term potentiation and long-term depression (LTP/LTD). Cold Spring Harb. Perspect. Biol. 4, a005710.

Lüscher, C., Xia, H., Beattie, E.C., Carroll, R.C., von Zastrow, M., Malenka, R.C., and Nicoll, R.A. (1999). Role of AMPA receptor cycling in synaptic transmission and plasticity. Neuron 24, 649–658.

Lynch, G. (2006). Glutamate-based therapeutic approaches: Ampakines. Curr. Opin. Pharmacol. 6, 82–88.

Ma, T., and Klann, E. (2012). Amyloid β: linking synaptic plasticity failure to memory disruption in Alzheimer's disease. J. Neurochem. 120, 140–148.

Mak, A.B., Pehar, M., Nixon, A.M.L., Williams, R.A., Uetrecht, A.C., Puglielli, L., and Moffat, J. (2014). Post-translational regulation of CD133 by ATase1/ATase2-mediated lysine acetylation. J. Mol. Biol. 426, 2175–2182.

Makino, H., and Malinow, R. (2009). AMPA receptor incorporation into synapses during LTP: the role of lateral movement and exocytosis. Neuron 64, 381–390.

Malinow, R., and Malenka, R.C. (2002). AMPA receptor trafficking and synaptic plasticity. Annu. Rev. Neurosci. 25, 103–126.

Marttinen, M., Takalo, M., Natunen, T., Wittrahm, R., Gabbouj, S., Kemppainen, S., Leinonen, V., Tanila, H., Haapasalo, A., and Hiltunen, M. (2018). Molecular mechanisms of synaptotoxicity and neuroinflammation in Alzheimer's disease. Front. Neurosci. 12, 963.

McClean, P.L., and Hölscher, C. (2014). Liraglutide can reverse memory impairment, synaptic loss and reduce plaque load in aged APP/PS1 mice, a model of Alzheimer's disease. Neuropharmacology 76, 57–67.

Miller, E.C., Teravskis, P.J., Dummer, B.W., Zhao, X., Huganir, R.L., and Liao, D. (2014). Tau phosphorylation and tau mislocalization mediate soluble Aβ oligomer-induced AMPA glutamate receptor signaling deficits. Eur. J. Neurosci. 39, 1214–1224.

Miñano-Molina, A.J., España, J., Martín, E., Barneda-Zahonero, B., Fadó, R., Solé, M., Trullás, R., Saura, C.A., and Rodríguez-Alvarez, J. (2011). Soluble oligomers of amyloid-β peptide disrupt membrane trafficking of α-amino-3-hydroxy-5-methylisoxazole-4-propionic acid receptor contributing to early synapse dysfunction. J. Biol. Chem. 286, 27311–27321.

Miyamoto, T., Kim, D., Knox, J.A., Johnson, E., and Mucke, L. (2016). Increasing the receptor tyrosine kinase EphB2 prevents amyloid-β-induced depletion of cell surface glutamate receptors by a mechanism that requires the PDZ-binding motif of EphB2 and neuronal activity. J. Biol. Chem. 291, 1719–1734.

Monteiro-Fernandes, D., Silva, J.M., Soares-Cunha, C., Dalla, C., Kokras, N., Arnaud, F., Billiras, R., Zhuravleva, V., Waites, C., Bretin, S., et al. (2020). Allosteric modulation of AMPA receptors counteracts Tau-related excitotoxic synaptic signaling and memory deficits in stress- and Aβ-evoked hippocampal pathology. Mol. Psychiatry. https://doi.org/10.1038/s41380-020-0794-5.

Moraes, B.J., Coelho, P., Fão, L., Ferreira, I.L., and Rego, A.C. (2020). Modified glutamatergic postsynapse in neurodegenerative disorders. Neuroscience. https://doi.org/10.1016/j.neuroscience.2019.12.002.

Nabavi, S., Fox, R., Proulx, C.D., Lin, J.Y., Tsien, R.Y., and Malinow, R. (2014). Engineering a memory with LTD and LTP. Nature 511, 348–352.

Oddo, S., Caccamo, A., Shepherd, J.D., Murphy, M.P., Golde, T.E., Kayed, R., Metherate, R., Mattson, M.P., Akbari, Y., and LaFerla, F.M. (2003). Triple-transgenic model of Alzheimer's Disease with plaques and tangles: intracellular Aβ and synaptic dysfunction. Neuron 39, 409–421.

Opazo, P., Viana da Silva, S., Carta, M., Breillat, C., Coultrap, S.J., Grillo-Bosch, D., Sainlos, M., Coussen, F., Bayer, K.U., Mulle, C., et al. (2018). CaMKII metaplasticity drives Aβ oligomer-mediated synaptotoxicity. Cell Rep. 23, 3137–3145.

Palop, J.J., and Mucke, L. (2010). Amyloid-B-induced neuronal dysfunction in Alzheimer's disease: from synapses toward neural networks. Nat. Neurosci. 13, 812–818.

Parameshwaran, K., Dhanasekaran, M., and Suppiramaniam, V. (2008). Amyloid beta peptides and glutamatergic synaptic dysregulation. Exp. Neurol. 210, 7–13.

Parkinson, G.T., and Hanley, J.G. (2018). Mechanisms of AMPA receptor endosomal sorting. Front. Mol. Neurosci. 11, 440.

Paula-Lima, A.C., Brito-Moreira, J., and Ferreira, S.T. (2013). Deregulation of excitatory neurotransmission underlying synapse failure in Alzheimer's disease. J. Neurochem. 126, 191–202.

Rajmohan, R., and Reddy, P.H. (2017). Amyloid-Beta and phosphorylated tau accumulations cause abnormalities at synapses of Alzheimer's disease neurons. J. Alzheimers Dis. 57, 975–999.

Reinders, N.R., Pao, Y., Renner, M.C., da Silva-Matos, C.M., Lodder, T.R., Malinow, R., and Kessels, H.W. (2016). Amyloid-β effects on synapses and memory require AMPA receptor subunit GluA3. Proc. Natl. Acad. Sci. U S A 113, E6526–E6534.

Reiserer, R.S., Harrison, F.E., Syverud, D.C., and McDonald, M.P. (2007). Impaired spatial learning in the APP Swe + PSEN1ΔE9 bigenic mouse model of Alzheimer's disease. Genes Brain Behav. 6, 54–65.

Rodrigues, E.M., Scudder, S.L., Goo, M.S., and Patrick, G.N. (2016). Aβ-induced synaptic alterations require the E3 ubiquitin ligase nedd4-1. J. Neurosci. 36, 1590–1595.

Roselli, F., Tirard, M., Lu, J., Hutzler, P., Lamberti, P., Livrea, P., Morabito, M., and Almeida, O.F.X. (2005). Soluble β-amyloid1-40 induces NMDA-dependent degradation of postsynaptic density-95 at glutamatergic synapses. J. Neurosci. 25, 11061–11070.

Rotte, A., Bhandaru, M., Cheng, Y., Sjoestroem, C., Martinka, M., and Li, G. (2013). Decreased expression of nuclear p300 is associated with disease progression and worse prognosis of melanoma patients. PLoS One 8, e75405.

Samra, A., and Ramtahal, J. (2012). Recurrent subacute visual loss presenting in a 52-year-old Caucasian woman with chronic relapsing inflammatory optic neuropathy: a case report. Brain 139, 16–17.

Sánchez-Rodríguez, I., Djebari, S., Temprano-Carazo, S., Vega-Avelaira, D., Jiménez-Herrera, R., Iborra-Lázaro, G., Yajeya, J., Jiménez-Díaz, L., and Navarro-López, J.D. (2019). Hippocampal long-term synaptic depression and memory deficits induced in early amyloidopathy are prevented by enhancing G-protein-gated inwardly rectifying potassium channel activity. J. Neurochem. 153, 362.

Schwarz, L.A., Hall, B.J., and Patrick, G.N. (2010). Activity-dependent ubiquitination of GluA1 mediates a distinct AMPA receptor endocytosis and sorting pathway. J. Neurosci. 30, 16718–16729.

Sebti, S., Prébois, C., Pérez-Gracia, E., Bauvy, C., Desmots, F., Pirot, N., Gongora, C., Bach, A.S., Hubberstey, A.V., Palissot, V., et al. (2014). BAT3 modulates p300-dependent acetylation of p53 and autophagy-related protein 7 (ATG7) during autophagy. Proc. Natl. Acad. Sci. U S A 111, 4115–4120.

Selkoe, D.J. (2002). Alzheimer's disease is a synaptic failure. Science 298, 789–791.

Selkoe, D.J., and Hardy, J. (2016). The amyloid hypothesis of Alzheimer's disease at 25 years. EMBO Mol. Med. 8, 595–608.

Shankar, G.M., Li, S., Mehta, T.H., Garcia-Munoz, A., Shepardson, N.E., Smith, I., Brett, F.M., Farrell, M.A., Rowan, M.J., Lemere, C.A., et al. (2008). Amyloid-β protein dimers isolated directly from Alzheimer's brains impair synaptic plasticity and memory. Nat. Med. 14, 837–842.

Sheng, M., Sabatini, B.L., and Südhof, T.C. (2012). Synapses and Alzheimer's disease. Cold Spring Harb. Perspect. Biol. 4, 10.

Shepherd, J.D., and Huganir, R.L. (2007). The cell biology of synaptic plasticity: AMPA receptor trafficking. Annu. Rev. Cell Dev. Biol. 23, 613–643.

Shi, D., Pop, M.S., Kulikov, R., Love, I.M., Kung, A.L., Kung, A., and Grossman, S.R. (2009). CBP and p300 are cytoplasmic E4 polyubiquitin ligases for p53. Proc. Natl. Acad. Sci. U S A 106, 16275–16280.

Shi, Q., Chowdhury, S., Ma, R., Le, K.X., Hong, S., Caldarone, B.J., Stevens, B., and Lemere, C.A. (2017). Complement C3 deficiency protects against neurodegeneration in aged plaque-rich APP/PS1 mice. Sci. Transl. Med. 9, eaaf6295.

Da Silva, S.V., Haberl, M.G., Zhang, P., Bethge, P., Lemos, C., Gonçalves, N., Gorlewicz, A., Malezieux, M., Gonçalves, F.Q., Grosjean, N., et al. (2016). Early synaptic deficits in the APP/PS1 mouse model of Alzheimer's disease involve neuronal adenosine A2A receptors. Nat. Commun. 7, 11915.

Song, I., and Huganir, R.L. (2002). Regulation of AMPA receptors during synaptic plasticity. Trends Neurosci. 25, 578–588.

Styr, B., and Slutsky, I. (2018). Imbalance between firing homeostasis and synaptic plasticity drives early-phase Alzheimer's disease. Nat. Neurosci. 21, 463–473.

Sun, H., Liu, M., Sun, T., Chen, Y., Lan, Z., Lian, B., Zhao, C., Liu, Z., Zhang, J., and Liu, Y. (2019). Age-related changes in hippocampal AD pathology, actin remodeling proteins and spatial memory behavior of male APP/PS1 mice. Behav. Brain Res. 376, 112182.

Swanson, G.T. (2009). Targeting AMPA and kainate receptors in neurological disease: therapies on the horizon? Neuropsychopharmacology 34, 249–250.

Tanaka, H., Sakaguchi, D., and Hirano, T. (2019). Amyloid-β oligomers suppress subunit-specific glutamate receptor increase during LTP. Alzheimers Dement. Transl. Res. Clin. Interv. 5, 797–808.

Thomas, M.H., Paris, C., Magnien, M., Colin, J., Pelleïeux, S., Coste, F., Escanyé, M.C., Pillot, T., and Olivier, J.L. (2017). Dietary arachidonic acid increases deleterious effects of amyloid-β oligomers on learning abilities and expression of AMPA receptors: putative role of the ACSL4-cPLA2 balance. Alzheimers Res. Ther. 9, 69.

Thorns, V., Mallory, M., Hansen, L., and Masliah, E. (1997). Alterations in glutamate receptor 2/3 subunits and amyloid precursor protein expression during the course of Alzheimer's disease and Lewy body variant. Acta Neuropathol. 94, 539–548.

Ting, J.T., Kelley, B.G., Lambert, T.J., Cook, D.G., and Sullivan, J.M. (2007). Amyloid precursor protein overexpression depresses excitatory transmission through both presynaptic and postsynaptic mechanisms. Proc. Natl. Acad. Sci. U S A 104, 353–358.

Tramutola, A., Triani, F., Di Domenico, F., Barone, E., Cai, J., Klein, J.B., Perluigi, M., and Butterfield, D.A. (2018). Poly-ubiquitin profile in Alzheimer disease brain. Neurobiol. Dis. 118, 129–141.

Trinchese, F., Liu, S., Battaglia, F., Walter, S., Mathews, P.M., and Arancio, O. (2004). Progressive age-related development of Alzheimer-like pathology in APP/PS1 mice. Ann. Neurol. 55, 801–814.

Trzepacz, P.T., Cummings, J., Konechnik, T., Forrester, T.D., Chang, C., Dennehy, E.B., Willis, B.A., Shuler, C., Tabas, L.B., and Lyketsos, C. (2013). Mibampator (LY451395) randomized clinical trial for agitation/aggression in Alzheimer's disease. Int. Psychogeriatrics 25, 707–719.

Vargas, J.Y., Fuenzalida, M., and Inestrosa, N.C. (2014). In vivo activation of Wnt signaling pathway enhances cognitive function of adult mice and reverses cognitive deficits in an Alzheimer's disease model. J. Neurosci. 34, 2191–2202.

Vyas, Y., Montgomery, J.M., and Cheyne, J.E. (2020). Hippocampal deficits in amyloid-β-related rodent models of Alzheimer's disease. Front. Neurosci. 14, 266.

Wakabayashi, K., Narisawa-Saito, M., Iwakura, Y., Arai, T., Ikeda, K., Takahashi, H., and Nawa, H. (1999). Phenotypic down-regulation of glutamate receptor subunit GluR1 in Alzheimer's disease. Neurobiol. Aging 20, 287–295.

Walsh, D.M., Klyubin, I., Fadeeva, J.V., Cullen, W.K., Anwyl, R., Wolfe, M.S., Rowan, M.J., and Selkoe, D.J. (2002). Naturally secreted oligomers of amyloid β protein potently inhibit hippocampal long-term potentiation in vivo. Nature 416, 535–539.

Wang, D., Yuen, E.Y., Zhou, Y., Yan, Z., and Xiang, Y.K. (2011). Amyloid β peptide-(1 - 42) induces internalization and degradation of β 2 adrenergic receptors in prefrontal cortical neurons. J. Biol. Chem. 286, 31852–31863.

Wang, G., Li, S., Gilbert, J., Gritton, H.J., Wang, Z., Li, Z., Han, X., Selkoe, D.J., and Man, H.-Y. (2017). Crucial roles for SIRT2 and AMPA receptor acetylation in synaptic plasticity and memory. Cell Rep. 20, 1335–1347.

Ward, S.E., Bax, B.D., and Harries, M. (2010). Challenges for and current status of research into positive modulators of AMPA receptors. Br. J. Pharmacol. 160, 181–190.

Wezenberg, E., Jan Verkes, R., Ruigt, G.S.F., Hulstijn, W., and Sabbe, B.G.C. (2007). Acute effects of the ampakine farampator on memory and information processing in healthy elderly volunteers. Neuropsychopharmacology 32, 1272–1283.

Wisniewski, M.L., Hwang, J., and Bahr, B.A. (2011). Submicromolar Aβ42 reduces hippocampal glutamate receptors and presynaptic markers in an aggregation-dependent manner. Biochim. Biophys. Acta 1812, 1664–1674.

Yasuda, R.P., Ikonomovic, M.D., Sheffield, R., Rubin, R.T., Wolfe, B.B., and Armstrong, D.M. (1995). Reduction of AMPA-selective glutamate receptor subunits in the entorhinal cortex of patients with Alzheimer's disease pathology: a biochemical study. Brain Res. 678, 161–167.

Yu, W., and Lu, B. (2012). Synapses and dendritic spines as pathogenic targets in Alzheimer's disease. Neural Plast. 2012, 247150.

Zhang, B., Li, Y., Liu, J.-W., Liu, X.-W., Wen, W., Cui, Y., and Huang, S.-M. (2019). Postsynaptic GluR2 involved in amelioration of Ab-induced memory dysfunction by KAIXIN-San through rescuing hippocampal LTP in mice. Rejuvenation Res. 22, 131–137.

Zhang, D., Hou, Q., Wang, M., Lin, A., Jarzylo, L., Navis, A., Raissi, A., Liu, F., and Man, H.Y. (2009). Na, K-ATPase activity regulates AMPA receptor turnover through proteasome-mediated proteolysis. J. Neurosci. 29, 4498–4511.

Zhang, J., Yin, Y., Ji, Z., Cai, Z., Zhao, B., Li, J., Tan, M., and Guo, G. (2017). Endophilin2 interacts with GluA1 to mediate AMPA receptor endocytosis induced by oligomeric amyloid-β. Neural Plast. 2017, 8197085.

Zhang, Y., Kurup, P., Xu, J., Anderson, G.M., Greengard, P., Nairn, A.C., and Lombroso, P.J. (2011). Reduced levels of the tyrosine phosphatase STEP block beta amyloid-mediated GluA1/GluA2 receptor internalization. J. Neurochem. 119, 664–672.

Zhang, Y., Guo, O., Huo, Y., Wang, G., and Man, H.-Y. (2018). Amyloid-B induces AMPA receptor ubiquitination and degradation in primary neurons and human brians of Alzheimer's disease. J. Alzheimer's Dis. 62, 1789–1801.

Zhao, L.-X., Chen, M.-W., Qian, Y., Yang, Q.-H., Ge, Y.-H., Chen, H.-Z., and Qiu, Y. (2019). M1 muscarinic receptor activation rescues β-amyloid-induced cognitive impairment through AMPA receptor GluA1 subunit. Neuroscience 408, 239–247.

Zhao, W.-Q., Santini, F., Breese, R., Ross, D., Zhang, X.D., Stone, D.J., Ferrer, M., Townsend, M., Wolfe, A.L., Seager, M.A., et al. (2010). Inhibition of calcineurin-mediated endocytosis and alpha-amino-3-hydroxy-5-methyl-4-isoxazolepropionic acid (AMPA) receptors prevents amyloid beta oligomer-induced synaptic disruption. J. Biol. Chem. 285, 7619–7632.

Zhu, J., and Tsai, N.P. (2020). Ubiquitination and E3 ubiquitin ligases in rare neurological diseases with comorbid epilepsy. Neuroscience 428, 90–99.

Supplemental Information

Acetylation of AMPA Receptors Regulates

Receptor Trafficking and Rescues Memory

Deficits in Alzheimer's Disease

Margaret O'Connor, Yang-Ping Shentu, Guan Wang, Wen-Ting Hu, Zhen-Dong Xu, Xiao-Chuan Wang, Rong Liu, and Heng-Ye Man

Figure S1

Figure S1. Injection of AAV-GluA1 in APP/PS1 mice increases GluA1 expression levels in the cortex. Related to Figure 5.

(A) GluA1, GluA2, synapsin I, synaptophysin, and PSD95 levels were detected by Western blotting in mouse cortex. GAPDH was used as a loading control. (n = 3 per group). **(B)** Quantification shows a reduction in synaptic marker proteins in APP/PS1 animals with an increase in GluA1 from AAV injection of GluA1-WT or GluA1-4KQ. **(C)** GluA1, GluA2, synapsin I, and PSD95 were detected by Western blotting in whole cell lysates, cytosolic fractions and synaptosomal fractions of mouse cortex. ** $p < 0.01$, *** $p < 0.001$. Data are mean ± SEM.

Figure S2

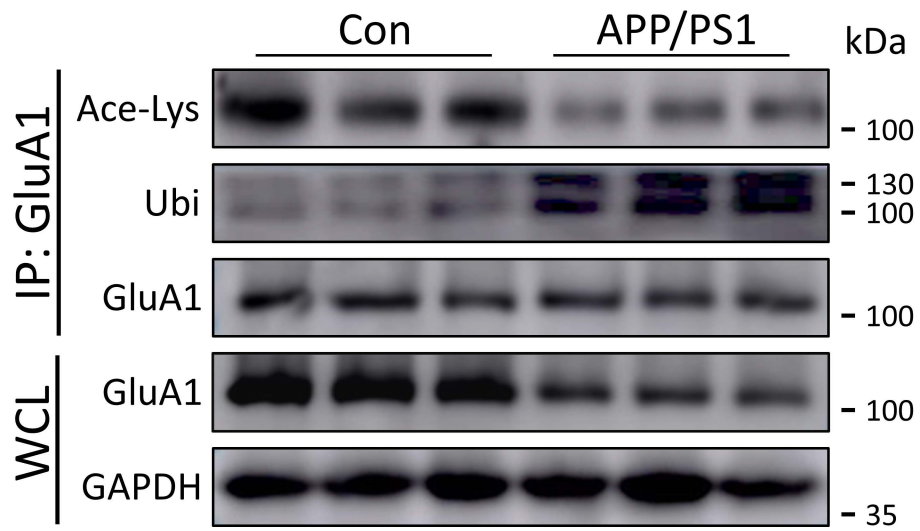**Figure S2. AMPAR acetylation impairments in 5-month-old APP/PS1 mice. Related to Figure 5.**

Hippocampal tissue from 5-month wild type and APP/PS1 mouse brains was homogenized and immunoprecipitated with antibody against GluA1. GluA1 acetylation and ubiquitination levels were detected through probing the immunoprecipitated GluA1 with anti-Acetyl-Lysine or ubiquitin antibodies, respectively. (*n* = 3 brains).

TRANSPARENT METHODS

Animal care and use

The Tg(APPswe,PSEN1dE9)85Dbo (APP/PS1) mice and littermates were from Jackson Lab. The mice were kept under standard laboratory conditions: 12 h light and 12 h dark with water and food ad libitum. All animal experiments were approved by the Animal Care and Use Committee of Huazhong University of Science and Technology, and performed in compliance with the National Institutes of Health Guide for the Care and Use of Laboratory Animals.

Human brain tissue use

Human brain tissues from control and AD patients were provided by, and used with approval from, the Boston University Alzheimer's Disease Center. Samples were collected from both males and females aged from 54 to 96 years old.

Intracerebroventricular viral injection

For AAV injection, the APP/PS1 mice were deeply anesthetized with isoflurane; AAV particles (1.0 μL at 0.1 μL/min) were injected into the lateral ventricle (1.8 mm antero-posterior, 1.06 mm medio-lateral, 2 mm dorso-ventral). After the injection, the mice were placed on a heating plate for recovery, and then were kept under standard laboratory conditions. The AAV of Control, GluA1-WT and GluA1-4KQ were constructed and prepared by Obio Technology (Shanghai, China).

Preparation of primary neuron culture

Cortical and hippocampal brain tissues were dissected out from embryonic day 18 (E18) rats of either sex to be used for primary culture. Tissues were digested at 37°C with papain (0.5 mg/mL in HBSS) for 20 min and titrated to completely dissociate neurons with titration buffer (0.1% DNase [cat. # PA5-22017 RRID: AB_11153259], 1% ovomucoid [Sigma-Aldrich; cat. # T2011]/1% bovine serum albumin [Sigma-Aldrich; cat. #05470] in Dulbecco's modified Eagle's medium). Neurons were counted and plated on 18-mm circular coverslips (Carolina, Burlington, NC; cat. # 633013, No. 0) in 60-mm Petri dishes (five coverslips/dish). These coverslips were prepared with a coat of poly-L-lysine (Sigma-Aldrich; cat. # P2636; 100 µg/ml in borate buffer) overnight at 37°C which was washed three times with sterile deionized water. Neurons were plated in plating medium ((minimum essential media [MEM] containing 10% fetal bovine serum (Atlanta Biologicals, Flowery Branch, GA; cat. # S11550), 5% horse serum (Atlanta Biologicals; cat. # S12150), 31 mg L-cysteine, 1% penicillin/streptomycin (Corning, Corning, NY; cat. # 30-002-Cl), and L-glutamine (Corning; cat. # 25-005-Cl)) which was replaced 24 h later by feeding medium (Neurobasal medium supplemented with 1% HS, 2% B-27, and 1% penicillin/streptomycin and L-glutamine). Thereafter, neurons were maintained in feeding medium to which 5′-fluoro-2′-deoxyuridine (10 µm; Sigma-Aldrich; cat. # F0503) was supplemented at 7 d *in vitro* (DIV 7) to suppress glial growth. Animal procedures for neuronal cultures were in compliance with the policies of the Institutional Animal Care and Use Committee (IACUC) at Boston University.

Preparation and use of Aβ peptides

β-Amyloid (Aβ) [1-42] oligomeric peptides (Invitrogen, cat # 03-112) were prepared according to manufacturer's instructions. Briefly, lyophilized peptide was dissolved in HPLC grade water and diluted to 1 mg/ml with phosphate buffered saline (PBS). Peptides were then incubated at 37°C for at least 24 h. Aliquots were made and stored at -20°C. Aliquots were thawed once directly prior to use. Neuronal cultures were treated with Aβ oligomers or water at a comparable volume as a control.

Transfection

Neurons at DIV 8-12 or HEK 293T cells that were split and cultured overnight were transfected with lipofectamine 2000 (Life Technologies) along with the target plasmids. Lipofectamine 2000 was mixed with target plasmids in 1X Dulbecco's Modified Eagle's Medium (DMEM, Corning) for 20 minutes at room temperature to form the transfection complex. The transfection complex was then incubated with the cells in culture medium for another 3-4-h at 37℃ in the cell culture incubator. Afterward, the medium with the transfection complex was replaced with fresh culture medium. For neurons, half of the fresh feeding medium was supplemented with conditioned feeding medium to minimize cell death. HEK 293T cells were cultured in the following medium: 1X DMEM with 10% FBS, 1% P/S and 1% L-Glutamine. To exogenously express the GluA1 subunit of AMPARs in HEK cells, a pRK5 plasmid vector carrying GluA1-GFP cDNA was transfected and then incubated for another 48 h before further experiments.

Immunocytochemistry of cultured neurons

Hippocampal neurons were washed in ice-cold artificial cerebral spinal fluid (aCSF (140 mM NaCl, 3 mM KCl, 10 mM HEPES, 2 mM $CaCl_2$, 1 mM $MgCl_2$, and 10 mM glucose)) and fixed for 8 min in a 4% paraformaldehyde/4% sucrose solution at room temperature. Cell membranes were permeabilized for 5 min in 0.3% Triton-X-100 (Fisher Biotech) in phosphate buffered saline (PBS), rinsed three times in PBS, then blocked for 1 h in 5% goat serum in PBS. After blocking, cells were incubated with primary antibodies (in 5% goat serum PBS) for 2 h at room temperature, then washed with PBS and incubated with Alexa Fluor-conjugated fluorescent secondary antibodies (1:500, Life Technologies) for 1 h at room temperature. Cells were then mounted to microscopy glass slides with Prolong Gold anti-fade mounting reagent (Life Technologies) for subsequent visualization.

Internalization assay

After drug treatment, neurons were incubated with GluA1Nt antibody (Neuromab, 1:100) or GFP antibody (Synaptic Systems, 1:100) for GluA1-4KQ-GFP experiments at 37°C for 10 min and then washed twice with feeding medium to get rid of extra antibody. After replacing the treatment with the cells' original culture medium, cells were placed in the incubator for 20 min. Neurons were then fixed in 4% paraformaldehyde/4% sucrose solution for 8 min. Neurons were blocked with 10% GS and further incubated with a secondary antibody (Alexa Fluor dye 488 or HRP, 1:500, 1 h) to bind all the AMPARs remaining on the cell surface. Neurons were permeabilized with 0.3% Triton X-100/PBS for 5 min, blocked in 10% goat serum for 1 h and incubated with another secondary antibody of a different color (Alexa Fluor dye 555, 1:500, 1 h) to specifically label the

internalized AMPARs. Quantitation of the GluA1 puncta was performed in ImageJ. A threshold was set to all the cell pictures so that all the GluA1 puncta were marked.

GST assay

The GST assay was adapted from Einarson et al., 2007. The BL21 *E.coli* bacteria were transformed with GST-GluA1-Cterm plasmid then grown at 37°C to show single colonies (diameter <1mm) before the experiments. For each experiment, one colony of transformed BL21 bacteria was inoculated into 2-ml aliquot of LB containing appropriate antibiotic selection then grew overnight at 37°C with shaking at 250 rpm. One liter of LB containing the antibiotic selection was then inoculated with the 2-mL aliquot of transformed BL21 bacteria and grown at 19°C with shaking for a few hours untill the OD600 reached 0.5-1.0. Isopropyl β-D-1-thiogalactopyran (IPTG) was then added to the concentration of 0.1 mM to induce the expression of GST-GluA1-Cterm recombinant protein for another 3 hours. The bacteria were centrifuged at 3500 g for 20 min at 4°C to be concentrated then lysed in 20 mL of PBS for lysis with repeated sonication. Lysed bacteria were centrifuged again at 12,000 g for another 15 min at 4°C to keep the supernatant. GST-GluA1-Cterm recombinant protein in the supernatant was then purified with GST beads and resuspended in acetylation assay buffer [RIPA buffer (50 mM Tris-HCl pH 7.4, 150 mM NaCl, 1% NP-40, 1% SDOC, and 0.1% SDS) supplemented with a protease inhibitor cocktail (Roche, cat# 11697498001) and a protein deacetylase inhibitor cocktail (100 mM trichostatin A, 50 mM sodium butyrate, and 50 mM nicotinamide)]. Resuspended GST beads were equally divided into several aliquots for protein acetylation assay.

Western blotting

Cultured neurons were lysed in Laemmli 2X sample buffer (4% SDS, 10% 2-mercaptoethanol, 20% glycerol, 0.004% bromophenol blue, 0.125 M Tris HCl) and boiled for 15 min at 95°C and then stored at -20°C. Mouse brain hippocampal tissues were boiled at 100°C for 5 min in the loading buffer (50 mM Tris-HCl, pH 7.6, 2% SDS, 10% glycerol, 10 mM DTT, and 0.2% bromophenol blue). Proteins in cell lysates of brain homogenates were separated using SDS-PAGE gels and transferred to polyvinylidene fluoride (PVDF) membranes. Membranes were blocked with 10% milk in Tris buffered saline supplemented with 0.05% Tween (TBST) for 1 h at room temperature. After blocking, membranes were incubated with primary antibodies (in 5% milk in TBST) overnight at 4°C. Membranes were washed 3x in TBST for 5-10 min and then incubated with a secondary antibody tagged with horse radish peroxidase (HRP) for 1 h at room temperature. Membranes were washed 3x with TBST and visualized using a chemiluminescence detection system (GE Healthcare) and exposed on Fuji medical X-ray films (Fisher Scientific). The film was scanned and analyzed using ImageJ.

Immunoprecipitation

Cultured neurons or brain tissues were lysed on ice in 1x radioimmunoprecipitation assay (RIPA) buffer (50 mM Tris-HCl [pH 7.4], 50 mM NaCl, 1% NP-40, 1% sodium deoxycholate [SDoC], and 0.1%-1% SDS) supplemented with protease inhibitor cocktail tablets (11697498001, Roche) to reduce protein degradation. For IP experiments, stringent RIPA buffer (1% SDS) was used to ensure specificity of immunoprecipitation.

For co-IP experiments, mild RIPA buffer (0.1% SDS) was used to preserve protein-protein interactions. After collection, cells were lysed by pipetting, followed by 5 bursts of sonication. Samples were then rotated head-to-toe for 30 min and centrifuged at 13,000 rpm at 4°C for 20 min. The protein concentration of the supernatant was balanced using a BCA assay while the pellets were discarded. A small portion of each sample was saved as a total cell lysate while the remainder was incubated with specific antibodies for 1 h, rotating, at 4°C, then incubated overnight after the addition of protein A-agarose beads (sc-2001, Santa Cruz Biotechnology). Agarose beads were rinsed at least three times with the lysis buffer used for that assay. The samples were finally boiled with Laemmli 2X sample buffer (4% SDS, 10% 8 2-mercaptoethanol, 20% glycerol, 0.004% bromophenol blue, and 0.125 M Tris HCl) for 10-15 min at 95°C before being used in immunoblotting assays.

Post-translational modification assays

Acetylation assays were designed as in Wang et al., 2017, and ubiquitination assays as in Huo et al., 2015. To detect the post-translational modification signal of endogenous AMPARs in brain (*in vivo*) or neuronal culture (*in vitro*), the GluA1 subunit was first immunoprecipitated from whole-brain extracts or homogenized cortical neuron lysates following the Immunoprecipitation procedure described above, using a specific antibody bound by Protein A-agarose beads. Lysis buffer (RIPA buffer with 1% SDS) was used to homogenize the brain tissue. The buffer was supplemented with a cocktail of deacetylase inhibitors (100 μM trichostatin A, 50 mM sodium butyrate, and 50 mM nicotinamide), to sufficiently block deacetylase activity, and deubiquitination inhibitors (5 μM ubiquitin

aldehyde) as needed. The acetylation signal was then assessed by immunoblotting with an antibody that detects general acetylated lysine residues (1:1000; ab80178, Abcam or 32268, Santa Cruz). Ubiquitination signals were detected by immunoblotting with an antibody targeting ubiquitin (1:1000; ab19247, Abcam) and smear signals above 100 kDa were measured and quantified.

Synaptosome purification

For brain tissues, the hippocampus or cortex of APP/PS1 mice were washed with cool artificial cerebral spinal fluid (aCSF: 140 mM NaCl, 3 mM KCl, 10 mM HEPES, 2 mM $CaCl_2$, 1 mM $MgCl_2$, and 10 mM glucose) and suspended in 300 μL (per 30 mg tissue) solution A containing 0.32 M sucrose, 1 mM $NaHCO_3$, 1 mM $MgCl_2$, 0.5 mM $CaCl_2 \cdot 2H_2O$, 10 mM sodium pyrophosphate, and protease inhibitors on ice. The suspension was collected and mixed up and down with a pipette up to 12 times, centrifuged at 710 g for 10 min, and the supernatant was collected. The pellet (P1) was re-suspended in 50 mL of solution A, and following pipetting up and down three times, centrifuged at 1,400 g for 10 min. The supernatant was collected together with the previously collected supernatant as whole-cell lysate (S1, whole). S1 was further centrifuged at 13,800 g for 10 min; supernatant (S2, cytosolic fraction) and pellet (P2, containing synaptosome and mitochondria) were separated. Pellet was resuspended in RIPA buffer, sonicated on ice, and rotated at 4°C for 30 min. For cultured neurons, synaptic fractions were purified using Syn-PER Synaptic Protein Extraction Reagent (87793, Thermo Scientific). The protein concentrations in whole, cytosolic, and crude synaptosomal fractions were measured by

BCA assay. Samples were then boiled with 4X loading buffer for Western blotting detection.

Acute brain slice preparation and LTP recording

Mice were decapitated under anesthesia with isoflurane, the brain was quickly removed and placed in ice-cold oxygenated artificial cerebral spinal fluid (aCSF) containing 119 mM NaCl, 2.5 mM KCl, 26.2 mM $NaHCO_3$, 1 mM NaH_2PO_4, 11 mM glucose, 1.3 mM $MgSO_4$, and 2.5 mM $CaCl_2$ (pH 7.4). Horizontal 350 μm thick brain slices were cut in ice-cold aCSF using a vibrating microtome (Leica, VT1000S, Germany). Slices were transferred to a recovery chamber at least 1.5 h with oxygenated aCSF at room temperature until recordings were performed.

For LTP recording, acute brain slices were transferred to a recording chamber and submerged in aCSF. Slices were laid down in a chamber with an 8 × 8 microelectrode array (Parker Technology, China) on the bottom plane (each 50 × 50 μm in size, with an interpolar distance of 150 μm) and kept submerged in aCSF. Signals were acquired using the MED64 System (Alpha MED Sciences, Panasonic). The fEPSPs in CA1 neurons were recorded by stimulating CA3 neurons. LTP was induced by applying three trains of high-frequency stimulation (HFS; 100 Hz, 1s duration). The LTP magnitude was quantified as the percentage change in the fEPSP slope (10%–90%) taken during the 60 min interval after LTP induction.

Behavior tests

Novel objective recognition test (NORT)

The mice were put in to the arenas (50 cm × 50 cm ×50 cm wooden container) for 5 min to adapt to the empty arenas 24 h before the test. 70% ethanol was used to clean arenas between each habituation period. On the first training day, the mice re-entered the arenas from the same starting point and were granted 5 min to familiarize themselves with the A object and B object. The 70% ethanol was used to clean arenas and objects after each familiarization period. One hour after the familiarization period, B object was replaced with C object, and the mice were granted 5 min to explore both objects; Twenty-four hours after the familiarization period, C object was replaced with D object, and the mice were granted 5 min to explore both objects. The recognition index was calculated by TA/(TA+TB), TB/(TA+TB),TC/(TA+TC), TD/(TA+TD). The discrimination index was calculated by (TC-TA)/(TA+TC), (TD-TA)/(TA+TD). TA, TB, TC, TD were respectively the time mice exploring the object A, B, C, D.

Fear conditioning test (FCT)

The fear conditioning test paradigm was conducted in a conditioning chamber (33 cm × 33 cm × 33 cm) equipped with white board walls, a transparent front door, a speaker, and a grid floor. On day 1, mice were placed into the conditioning chamber and allowed free exploration for 2 minutes before the delivery of the conditioned stimulus (CS) tone (20 seconds, 80 dB, 2,000 Hz) paired with a foot-shock unconditioned stimulus (2 seconds, 0.80 mA) through a grid floor at the end of the tone. A total of 1 CS–US pairs with a 60-second intertrial interval (ITI) were presented to each animal in the training stage. The mouse was removed from the chamber one minute after foot-shock and placed back in its home cage. The contextual fear conditioning stage started 24 hours after the training

phase, when the animal was put back inside the conditioning chamber for 5 minutes. 1 hours after context test, the animal was put back into the same chamber with different contextual cues, including yellow and blue wall, smooth plastic floor and vinegar drops condition for 5 minutes. The tone fear conditioning stage started 1 hours after the different contextual stage. After 2 minutes of free exploration, the mouse was exposed to the exact same 3-CS tones with 20-second ITI in the training stage without the foot-shock. The freezing responses of the animals were recorded in every test.

Morris water maze test (MWM)

The Water Maze test contains acquisition training and probe trial. During the acquisition training, the mice were trained to find a submerged platform hidden 1 cm under water by using constant cues outside the pool. During each trial, mice had up to 60 s to find the hidden platform; otherwise, they would be guided to the platform and forced to stay on it for 20 s. Acquisition training contained four trials a day for four consecutive days. The probe trial is used to test the memory of animals. One hour or 48 hours after the last training, the hidden platform was removed and each mouse was allowed to swim freely for 60 s. The swimming pathway, escape latency of mice to find the hidden platform, and the time spending in the target quadrant were recorded by a digital device connected to a computer.

Microscopy

Mounted coverslips were stored in the dark at 4°C for no longer than 1 week before fluorescence microscopy. An inverted Carl Zeiss fluorescent microscope was used to

collect all the images with a 63× oil-immersion objective (numerical aperture 1.4) and AxioVision software (release 4.5). The microscope eyepiece was used to focus on neurons and the stage moved to center neurons in frame. The software was then used to switch the light path to the camera for image capture. The exposure duration of the camera was determined before any pictures were taken and was kept constant throughout imaging. The exposure duration was established manually by using a glow-scale lookup table to ensure that the fluorescence signal was within the full dynamic range, and the same exposure parameters were used throughout an experiment. For each experiment, images of at least 10 neurons per group were randomly taken and used for quantification. Images were collected in 8-bit grayscale for later quantification using NIH ImageJ software.

Statistical analysis

For Western blots: Data from multiple trials were averaged to obtain the mean for each experiment. Means from at least 3 independent experiments were averaged to obtain the standard error of the mean (SEM), as indicated by the error bars on the bar charts. Immunointensity of bands was measured using ImageJ. Bands of interest were normalized to a corresponding tubulin or GAPDH loading control in the same lane, or to the total amount of pulled-down protein for immunoprecipitation assays. In cases of data normalization, control conditions were normalized to 1 by dividing all conditions and their SEMs by the value of the control condition. Statistical analysis was performed using the two-population student's t test and one-way analysis of variance (ANOVA) with Tukey post-hoc test.

For ICC: In ImageJ, images were manually thresholded to select synaptic puncta. To obtain intensity values, raw integrated density measurements were acquired using the Analyze Particles function. Measurements from at least three segments of secondary dendrites from different neurites were analyzed to represent one neuron. In cases of data normalization, control conditions were normalized to 1 by dividing all conditions and their SEMs by the value of the control condition. Statistical analysis was performed using the two-population student's t test and one-way ANOVA with Tukey post-hoc test.

For behavioral tests: Five animals for each experimental group were trained and tested as above. Statistical analysis was performed using one-way ANOVA with Tukey post-hoc test.

All data are expressed as mean ± SEM and analyzed using GraphPad Prism 5 statistical software (USA, GraphPad Software). $p < 0.05$ is considered as statistically significant. p values are presented as $p > 0.05$ (ns, not significant), $* p < 0.05$, $** p < 0.01$, and $*** p < 0.001$.

SUPPLEMENTAL REFERENCES

Einarson, M.B., Pugacheva, E.N., Orlinick, J.R., 2007. Preparation of GST Fusion
Proteins. CSH Protoc. 2007, pdb.prot4738.

Huo, Y., Khatri, N., Hou, Q., Gilbert, J., Wang, G., Man, H.-Y., 2015. The
deubiquitinating enzyme USP46 regulates AMPA receptor ubiquitination and
trafficking. J. Neurochem. 134, 1067–1080.

Wang, G., Li, S., Gilbert, J., Gritton, H.J., Wang, Z., Li, Z., Han, X., Selkoe, D.J., Man,
H.-Y., 2017. Crucial Roles for SIRT2 and AMPA Receptor Acetylation in Synaptic
Plasticity and Memory. Cell Rep. 20, 1335–1347.